https://doi.org/10.5194/gmd-2020-322
Preprint. Discussion started: 22 December 2020

Geoscientific Model Development Discussions

Incorporating ^{15}N into the outputs of SMOKE version 4.6 as the emission input dataset for CMAQ version 5.2.1 for assessing the role emission sources plays in controlling the isotopic composition of NO_x, NO_y, and atmospheric nitrate

Huan Fang[†] *and Greg Michalski*[†‡]

[†]Department of Earth, Atmospheric, and Planetary Sciences Purdue University, 550 Stadium Mall Drive, West Lafayette, IN 47907, United States

[‡]Department of Chemistry, Purdue University, 560 Oval Drive, West Lafayette, IN 47907, United States

Correspondence: Huan Fang, fang63@purdue.edu

https://doi.org/10.5194/gmd-2020-322
Preprint. Discussion started: 22 December 2020

Geoscientific Model Development Discussions

Abstract

Nitrogen oxides (NO_x = nitric oxide (NO) + nitrogen dioxides (NO_2)) are important trace gases that affect atmospheric chemistry, air quality, and climate. Contemporary development of NO_x emissions inventories is limited by the understanding of the roles of vegetation (net NO_x source or net sink), gasoline and diesel in vehicle emissions, and application of NO_x emission control technologies. In this study, we used the nitrogen stable isotope composition of NO_x ($\delta^{15}N(NO_x)$) to resolve the uncertainties in NO_x emission sources, by incorporating ^{15}N into the US EPA trace gas emission model SMOKE (Sparse Matrix Operator Kernel Emissions) and compared simulated spatiotemporal patterns in NO_x isotopic composition with corresponding atmospheric measurements in West Lafayette, Indiana, USA. The results indicate the potential underestimation of emissions from soil, livestock waste, off-road vehicles, and natural gas power plants and the potential overestimation of emissions from on-road vehicles and coal-fired power plants.

1. Introduction

NO_x are important trace gases that affect atmospheric chemistry, air quality, and climate (NO_x = nitric oxide (NO) + nitrogen dioxide (NO_2)). The main sources of tropospheric NO_x are emissions from vehicles, power plants, agriculture, livestock waste, as well as the natural by-product of nitrification and denitrification occurring in soil, and lightning. The NO_x photochemical cycle generates OH and HO_2 radicals, organic peroxy radicals (RO_2), and ozone (O_3), which ultimately oxidize NO_x into NO_y ($NO_y = NO_x + HONO + HNO_3 + HNO_4 + N_2O_5$ + other N oxides). During the photochemical processes that convert NO_x to NO_y, ground-level concentrations of O_3 become elevated and secondary particles are generated. Secondary aerosols in turn affect cloud physics, enhancing the reflection of solar radiation (Schwartz, 1996) and are hazardous to human health (Lighty et al., 2000). Thus, the importance of NO_x in air quality, climate, and human and environmental health makes understanding the spatial and temporal variation in the sources of NO_x a vital scientific question. However, despite years of research, there are still a number of significant uncertainties in the NO_x budget.

There are significant uncertainties in the amount of NO_x emitted by soil at local and global scales. About 15% of global NO_x emissions, ranging from 6.6 to 21 Tg N yr^{-1}, is derived from global soil NO_x emissions yet evaluating and verifying emission rates using both laboratory and field measurements is still a challenge (Galbally & Roy, 1978; Muller, 1992; Potter et al., 1996; Yienger and Levy, 1995; Davidson and Kingerlee, 1997; Ganzeveld et al., 2002; Jaeglé et al., 2005; Yan et al., 2005; Stehfest and Bouwman, 2006; Hudman et al., 2012). Soil NO_x emissions vary by different biome types, meteorological conditions, and soil physicochemical properties. Soil NO_x emissions also depend on soil moisture that is a function of climate, such as in Mediterranean climates and tropical savannas, where wet and dry seasons cause extreme fluctuations in soil moisture (Davidson, 1992; Yienger and Levy, 1995; Scholes et al., 1997; Zörner et al., 2016). The application of N fertilizer also has a strong effect on soil NO_x emissions, which can dramatically increase during the first 1-2 days after N fertilizer application and can take several weeks for the emission rate to drop to pre-fertilizer levels (Ludwig et al., 2001). N fertilizers nitrogen may have increased soil NO_x emissions by up to 11% (Shepherd, 1991; Pilegaard, 2013), and probably currently contributes 1.8 Tg N yr^{-1} (Hudman, 2012). Furthermore, soil NO_x emissions are likely to increase as the worldwide use of fertilizers grows (Galloway et al., 2004; Houlton et al., 2013). There is also a controversy about the fate of NO_x emitted by the soil in terms of the amount that escapes the canopy and mixes into the boundary layer. Previous research has highlighted the role

https://doi.org/10.5194/gmd-2020-322
Preprint. Discussion started: 22 December 2020

Geoscientific Model Development Discussions

of vegetation in NO_x removal, when the ambient NO_x concentrations are below the "compensation point" (i.e. between 1 and 3 ppbv), vegetation acts as a net source of atmospheric NO_x, but above 4 ppbv acts as a net sink (Johansson, 1987; Thoene, Rennenberg & Weber, 1996; Slovik et al., 1996; Webber & Rennenberg, 1996). However, other research claims the up to 75% of soil NO_x is lost through vegetation canopy reduction even when the ambient NO_x concentration was as low as 0.2 to 0.4 ppbv (Jacob & Wofsy, 1990; Hanson & Lindberg, 1991; Yienger & Levy II, 1995). For example, soil NO_x emission in California may be underestimated by up to 50% net due to the sink by vegetation, significantly changing current the NO_x emission inventory (Almaraz et al., 2018).

On-road vehicles are one of the major sources of NO_x, yet there are also questions about whether emission inventories are accurate. According to Parrish (2006), the estimation of on-road vehicle NO_x emission has at least 10 to 15% uncertainty. The algorithm used in the National Emission Inventory (NEI), is mileage-based, which estimates NO_x emission from on-road vehicles by travel time, speed of travel on different roadways, and emissions from vehicles per distance traveled. The emission factor of each vehicle classification and emission types are based on the represented measurement of NO_x from on-road vehicles in the US, under different ambient temperatures, travel speeds, operating modes, fuel volatility, and mileage accrual rates (Dreher & Harley, 1998; USEPA, 2003). However, the emission factors of vehicle classifications and emission types are derived from the measurements at a relatively small number of sites. As a result, the estimations of NO_x emission from on-road vehicles by mileage-based approach appears to be inconsistent with some on-road and ambient air measurements (Ingalls, 1989; Pierson et al., 1990; Fujita et al., 1992; Pierson et al., 1996; Singer and Harley, 1996). For example, NO_x emissions from diesel engines are likely underestimated by a factor of 2 (Pierson et al., 1996; Cicero-Fernandez et al., 1997; Sawyer et al., 2000) and estimates by the mileage-based approach does not follow the same spatial and temporal patterns as the NO_x measurements (Dreher & Harley, 1998). An alternative is a fuel-based approach, which directly uses to estimates fuel consumption based on gas tax data and derives the NO_x emission by the emission factors in gram per gallon based on the represented on-road measurements (Singer & Harley, 1996; Dreher & Harley, 1998). By doing so, the only uncertainties are fuel sales data and emission factors, which are easier to determine and get controlled. As a result, the emission inventories derived from the fuel-based approach are closer to the measurements (Singer & Harley, 1996; Dreher & Harley, 1998; Sawyer et al., 2000; Parrish, 2006). At the same time, however, the fuel-based approach fails to provide accurate spatial or temporal NO_x emissions (Sawyer et al., 2000).

The uncertainty in power plant NO_x emissions is mainly the result of the recent implementation of NO_x emission control technologies. The Clean Air Act of 1995 required NO_x emission control technologies to be implemented on new power plants. The major emission control technologies are a). LNB: low NO_x burner, which decreases NO_x emission by lowering the oxygen to nitrogen in the fuel; b). SCR: selective catalytic reduction, which chemically reduces NO_x to N_2 by using NH_3 or urea as a reductant over a metal catalyst; c). SNCR: selective non-catalytic reduction, converts NO_x to N_2 by reacting NO_x with NH_3 or urea; and d). OFA: over-fire air, which increases the fuel combustion efficiency by introducing air during the combustion (Felix et al., 2012; Srivastava et al., 2005; Xing et al., 2013). Between 1990 and 2010, In the United States, NO_x control technology used in coal-fired power plants increased from less than 20% to about 86%, and from less than 2% to 70% for natural gas power plants, which decreased overall US power plant NO_x emissions by about 70% (Xing et al., 2013). The reduction of NO_x emission from power plants varies by the facility, due to the choice of emission control technologies, which cause

https://doi.org/10.5194/gmd-2020-322
Preprint. Discussion started: 22 December 2020

Geoscientific Model Development Discussions

the uncertainties. The removal efficiencies of NO_x emission are also different for each control technology. LNB can remove up to 50% of NO_x emissions from power plants but using LNB and OFA at the same time could remove 60% to 75%. SNCR can remove 30% to 66% while SCR can remove 80% to more than 90% of power plant NO_x while reburning can remove 39% to 67% (Srivastava et al., 2005). All of these removal percentages, however, do not apply to initial fire-up times prior to catalyst efficiency reaching its maximum.

The nitrogen stable isotope composition of NO_x might be a useful tool to help resolve the uncertainties of how NO_x emission sources vary in space and time. Previous studies have shown that natural and anthropogenic NO_x sources have distinctive $^{15}N/^{14}N$ ratios (Ammann et al., 1999; Felix et al., 2012; Felix and Elliott, 2013; Fibiger et al., 2014; Heaton, 1987; Hoering, 1957; Miller et al., 2017; Walters et al., 2015a, 2015b, 2018). This variability in NO_x $^{15}N/^{14}N$ ratios quantified by

$$\delta^{15}N(NO_x)\ (‰) = [(^{15}NO_x/^{14}NO_x) / (^{15}N_2/^{14}N_2)_{air} - 1] \times 1000) \qquad \text{Eq. (1)}$$

where $^{15}NO_x/^{14}NO_x$ is the measurement of relative abundance of ^{15}N to ^{14}N in atmospheric NO_x, compared with the ratio of nitrogen in the air, which has a $^{15}N_2/^{14}N_2 = 0.0036$.

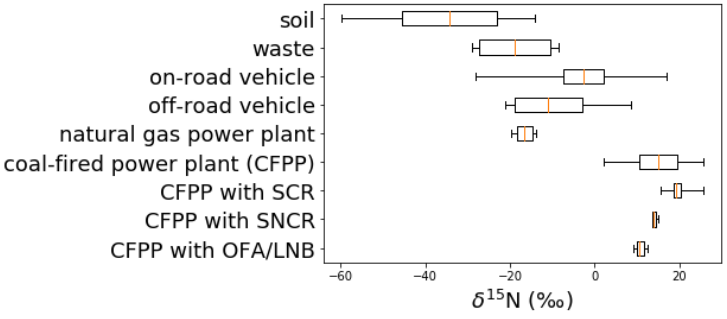

Figure 1: Box (lower quartile, median, upper quartile) and whisker (lower extreme, upper extreme) plot of the distribution of $\delta^{15}N$ values for various NO_x emission sources.

Previous research has shown that there are distinctive differences in $\delta^{15}N$ values for NO_x from different emission sources and significant variations within each source (Fig. 1). Soil NO_x has the lowest $\delta^{15}N$ values ranging from -59.8 ‰ to -19.8 ‰ (Li & Wang, 2008; Felix & Elliott, 2014; Yu & Elliott, 2017; Miller et al., 2018). The NO_x emission from waste has the second-lowest $\delta^{15}N$ values, ranging from -29 ‰ to -8.5 ‰ (Felix & Elliott, 2014). The NO_x emissions from vehicles are isotopically heavier relative to soil and waste, showing $\delta^{15}N$ values ranging from -19.2 ‰ to 17 ‰ (Moore, 1977; Heaton, 1990; Ammann et al., 1999; Pearson et al., 2000; Savard et al., 2009; Redling et al., 2013; Fibiger, 2014; Felix & Elliott, 2014; Walters et al., 2015a; Walters et al., 2015b). The NO_x emissions from natural gas power plants are also isotopically heavier than soil and waste, showing $\delta^{15}N$ values ranging from -19.7 ‰ to -13.9 ‰ (Walters et al., 2015b). The $\delta^{15}N$ values of NO_x emissions from coal-fired power plants have the highest values, ranging from 2.1 ‰ to 25.6 ‰ (Heaton, 1987; Heaton, 1990; Snape, 2003; Felix et al., 2012; Felix et al., 2015; Savard et al., 2017). The implement of emission control technology tends to increase NO_x $\delta^{15}N$ values. The $\delta^{15}N$ value of NO_x emitted from coal-fired power plant equipped with SCR ranges from 15.5 ‰ to 25.6 ‰ (Felix et al., 2012), the $\delta^{15}N$ of the NO_x emissions from coal-fired power plant equipped with SNCR ranges from 13.6 ‰ to 15.1 ‰ (Felix et al., 2012), the $\delta^{15}N$ of the NO_x

https://doi.org/10.5194/gmd-2020-322
Preprint. Discussion started: 22 December 2020

Geoscientific Model Development Discussions

emissions from coal-fired power plants equipped with OFA/LNB ranges from 9.0 ‰ to 12.6 ‰ (Felix et al., 2012). Similar isotope enrichment of NO_x has been noted in vehicles as their catalytic converters warm and become efficient (Walters et al, 2015a).

These distinctive differences in $\delta^{15}N$ values among different NO_x emission sources suggest $\delta^{15}N$ could be an effective tracer of atmospheric NO_x sources. For example, Redling et al. (2003) found higher $\delta^{15}N$ of NO_2 in samples collected closer to the highway compared to those adjacent to a forest, showing the emissions from vehicles were dominant near the highway. In addition, a strong positive correlation between the amount of NO_x emission from coal-fired power plants within 400 km radial area of study sites and $\delta^{15}N(NO_3^-)$ of wet and dry deposition has been demonstrated (Elliott et al., 2007; 2009). What is lacking is a systematic way of connecting $\delta^{15}N$ values of NO_x sources, regional emissions, and data from numerous studies to measurements of $\delta^{15}N$ in NO_y.

Here we have simulated the emission of $^{15}NO_x$ and compared the predicted $\delta^{15}N(NO_x)$ values with the recent measurements. The $\delta^{15}N$ values of atmospheric NO_x are impacted by three main factors. The first is the inherent variability of the $\delta^{15}N$ values of NO_x emissions in time and space. Secondly, atmospheric processes that mix the NO_x emissions, blurring multiple emission sources within a mixing lifetime relative to the NO_x chemical lifetime (~1 day). And thirdly, isotope effects occurring during tropospheric photochemistry may alter the $\delta^{15}N$ of NO_x emissions as they are transformed from NO_x into NO_y. In this paper, we first consider the effects from the first consideration, the variation in NO_x emission sources over time and space. In two companion papers, we will discuss the impacts from atmospheric mixing and tropospheric photochemistry by using the emission simulation presented here as the input dataset for the Community Multiscale Air Quality Modeling System (CMAQ) to simulate $\delta^{15}N$ of atmospheric NO_x. Thus, this research examines the variability in NO_x emissions over time and space in the Midwestern US and calculates ^{15}N emissions in order to predict the spatial and temporal changes of $\delta^{15}N$ values of emitted NO_x. The ultimate goal will be to evaluate the accuracy of the NO_x emission inventory using ^{15}N.

2. Methodology

The EPA trace gas emission model SMOKE (Sparse Matrix Operator Kernel Emissions) was used to simulate $^{14}NO_x$ and $^{15}NO_x$ emissions. $^{14}NO_x$ emissions we estimated using the SMOKE model based on NO_x emissions from 2002 NEI (National Emission Inventory, USEPA, 2014) emission sectors and ^{15}N emission were determined using these emissions and the corresponding $\delta^{15}N$ values of NO_x sources from previous research (Table 1). Using the definition of $\delta^{15}N$ (‰), $^{15}NO_x$ emitted by each SMOKE processing category (area, biogenic, mobile, and point) was calculated by

$$^{15}NO_x(i) = {}^{14}NO_x(i) \times {}^{15}R_{NO_x}(i) \quad \text{Eq. (2)}$$

where $^{14}NO_x$ (i) are the NO_x emissions for each category (i) obtained from NEI and SMOKE and $^{15}R_{NOxi}$ is a ^{15}N emission factor ($^{15}NO_{Xi}/^{14}NO_{xi}$) calculated by:

$$^{15}R_{NO_x}(i) = \left(\frac{\delta^{15}N_{NO_x}(i)}{1000} + 1\right) \times 0.0036 \quad \text{Eq. (3)}$$

$\delta^{15}N_{NOx(i)}$ is the $\delta^{15}N$ value of some NO_x source (i = area, biogenic, mobile, and point) and 0.0036 is the $^{15}N/^{14}N$ of air N_2, the reference point for $\delta^{15}N$ values. Thus, to use Eq. (2) we extended a

https://doi.org/10.5194/gmd-2020-322
Preprint. Discussion started: 22 December 2020

Geoscientific Model Development Discussions

NO_x emission dataset for the Midwestern US ($^{15}NO_x$ (i)) and used recent measurements to determine $\delta^{15}N_{NOx}$ values for major NO_x emission sources ($^{15}R_{NOxi}$) by using Eq. (3).

Annual emissions estimates by 2002 NEI for the Midwestern United States was obtained from NEI at the county-level and was converted into hourly emissions on a 12 km x 12 km grid over the Midwestern United States and previously published (Spak, Holloway, & Stone, 2007). The modeling domain includes latitudes between 37 º N and 45 º N, and longitudes between 98º W and 78º W, which fully covers the states of Minnesota, Iowa, Missouri, Wisconsin, Illinois, Michigan, Indiana, Kentucky, Ohio, and West Virginia, and partially covers North Dakota, South Dakota, Nebraska, Kansas, Tennessee, North Carolina, Virginia, Maryland, Pennsylvania, and New York. On-road gasoline, on-road diesel, off-road gasoline, off-road diesel, coal-fired power plant, natural gas power plant, soil, and livestock wastes are the main sources of NO_x emissions in the NEI (USEPA, 2014). These were imported into models that used parameters such as land use, plant species, temperature, growing season, plume rise, roadway type, vehicle classification, and travel time for vehicle emissions to convert them into hourly NO_x emissions. SMOKE categorizes NO_x emissions into four "processing categories": Biogenic, Mobile, Point, and Area (Table 1).

The choice of the 2002 version of NEI is, in part, arbitrary for several reasons. First, in order to compare the model estimated $\delta^{15}N$ values with observations, it requires the emission inventory to be relevant to the same timeframe as the $\delta^{15}N$ measurements of the NO_y. The data sets we compare to the model (discussed below) span the late 1990's to 2009, thus the 2002 inventory is more relevant than later inventories (2008 onward). Secondly, the current model is predicting the initial $\delta^{15}N$ value, but this value will be altered by two effects. First, the role of atmospheric transport and deposition, which will blur the regional $\delta^{15}N$ value of emissions based on emission strength, mixing vigor, and deposition schemes. Secondly, photochemical and equilibrium isotope effects that occur during the transformation of NO_x into NO_3^-, which is the most of the available NO_y $\delta^{15}N$ data, measured from either rain or aerosols. Thus, it was not expected that this current "emission only" model would accurately predict the $\delta^{15}N$ values of NO_3^-. Instead, the current work is a proof of concept paper that addresses some basic questions, for instance, do we expect regional and seasonal differences in $\delta^{15}N$ values of NO_x, and are they at least comparable to observations in NO_y? We emphasize that the effects of atmospheric mixing and tropospheric photochemistry will be addressed in subsequent papers.

SMOKE Processing Category	NEI Sector	$\delta^{15}N$-NO_x (‰) from previous research	$\delta^{15}N$-NO_x (‰) choose for this study
Biogenic	Soil	-59.8 ~ -14.0	-34.3 (Felix & Elliott, 2014)
Area	Livestock Waste	-29 ~ -8.5	-18.8 (Felix & Elliott, 2014)

https://doi.org/10.5194/gmd-2020-322
Preprint. Discussion started: 22 December 2020

Geoscientific Model Development Discussions

	Off-road Gasoline	-21.1 ~ 8.5	-11.5 (Walters et al., 2015b)
	Off-road Diesel		-10.5 (Walters et al., 2015b)
Mobile	On-road Gasoline	-28.1 ~ 17	-2.7 (Walters et al., 2015b)
	On-road Diesel		-2.5 (Walters et al., 2015b)
Point	Coal-fired Fossil Fuel Combustion	-19.7 ~ 25.6	15 (Felix et al., 2012)
	Natural Gas Fossil Fuel Combustion		-16.5 (Walters et al., 2015)

Table 1: The $\delta^{15}N$ values (in ‰) for NO_x emission sources based on SMOKE processing category and NEI sector

2.1 Biogenic source of NO_x emission

Biogenic sources of NO_x are predominately by-products of microbial nitrification and denitrification occurring in soil. The Biogenic Emissions Inventory System (BEIS) was implemented within SMOKE to estimate hourly emissions from biogenic sources. The normalized emission was first generated based on 230 land-use types from the Biogenic Emission Landcover Database (USEPA, 2018), a normalized emission factor of NO_x, and land cover, to indicate the emission under standard environmental conditions (at 30 °C and 1000 μmol m^{-2} s^{-1} photosynthetic active radiation). Then, meteorological data generated by MM5 (Fifth-Generation Penn State/NCAR Mesoscale Model) (Grell, Dudhia, & Stauffer, 1994) was incorporated into BEIS and was used to finalize the speciated and temporally allocated emissions from biogenic sources by the algorithm for NO_x. This algorithm uses three steps. First, the land surface was designated by the land use as agriculture and non-agriculture based on Biogenic Emission Landcover Database. Second, NO_x emissions were normalized based on temperature, precipitation, fertilizer application, and crop canopy coverage during the crop growing season (April 1 to October 31). Finally, for NO_x emissions over agriculture areas during the non-growing season and NO_x emissions over non-agriculture areas throughout the year, the emission NO_x factor was limited to that for grassland, and the only temperature was used to normalize NO_x emission (Pierce, 2001; Vukovich & Pierce, 2002; Schwede et al., 2005; Pouliot & Pierce, 2009; USEPA, 2018).

https://doi.org/10.5194/gmd-2020-322
Preprint. Discussion started: 22 December 2020

Geoscientific Model Development Discussions

The NO_x emission from the soil is regarded as a biogenic source in SMOKE, and there are only a few measurements of the $\delta^{15}N$ values of biogenic NO_x. Li & Wang (2008) measured the NO_x fluxes using dynamic flow chambers for 2 to 13 days after cropland soil was fertilized by either urea (n=9) or ammonium bicarbonate (n=9), and the $\delta^{15}N$ values of NO_x ranged from -48.9 ‰ to -19.8 ‰. Felix & Elliott (2014) placed a passive NO_2 sampler in a static flux chamber installed in a cornfield. NO_2 was continuously collected from Jun 19-22, 2010 after 135 kg N/ha of fertilizer was applied, and from Jun 2-19, 2011 after 40 kg N/ha of fertilizer application. The $\delta^{15}N$ values of NO_x emissions from these measurements range from -30.8 ‰ to -26.5 ‰. Miller et al. (2018) used a static flux chamber to collect soil NO_x emission 2~3 samples daily from May 17 to 26, 2016, and 2~4 samples daily from May 22 to Jun 3, 2017. The $\delta^{15}N$ values of NO_x emissions from these 37 samples ranged from -44.2 ‰ to -14.0 ‰. Yu & Elliott (2017) collected 15 samples from soil plots for the $\delta^{15}N$ value of NO flux over a fallow field 2 weeks after the precipitation. The $\delta^{15}N$ values of NO_x emissions from these measurements range from -59.8 ‰ to -23.4 ‰, with a standard deviation of ±11.25 ‰. The $\delta^{15}N$ values of NO_x emissions from soil wetted with NO_3^- aqueous solution treatments averaged -40.3 ± 0.75 ‰, while the $\delta^{15}N$ values of NO_x emissions from soil wetted with NO_2^- aqueous solution treatments averaged -29.1 ± 4.17 ‰ suggesting there are unique isotope effects for each step during $NO_3^- \rightarrow NO_2^- \rightarrow NO$ steps. The $\delta^{15}N$ values of NO_x emissions from soil wetted with NH_4^+ aqueous solution treatments averaged -57.8 ± 1.91 ‰, indicating $\delta^{15}N$ of NO_x derived from nitrification is different than that from denitrification. Based on these studies we adopted a $\delta^{15}N$ value for NO_x emissions from the soil of -34.3 ‰, which is the average value of these previous studies, to determine the emission rate of $^{15}NO_x$ from biogenic sources using Eq. (2) and (3).

2.2 Mobile source of NO_x emission

The emission of NO_x based on on-road vehicle activity was estimated using MOBILE6, a model developed by the EPA's Office of Transportation and Air Quality. There are three main factors that are considered to estimate on-road vehicle NO_x emissions. The first is the emission rate per mile traveled for 28 different classifications of vehicles. The second is the emission factor based on 10 different types of operating conditions (running, start, hot soak, diurnal, resting, run loss, crankcase, refueling, brake wear, and tire wear), travel speed over 33 different road types with distinct average speed, types of fuel being consumed, and ambient temperature. Finally, the number of vehicles in each classification, emission type, and fuel type along with each type of roadway during certain periods (USEPA, 2003; Houyoux, 2005). MOBILE6 and SMOKE were used to determine NO_x emissions along the roadways and were converted into hourly emissions within each 12 km × 12 km grid cell.

The NO_x emission from on-road vehicle employ an estimated $\delta^{15}N$ value from -28.1 ‰ to +17 ‰ (Moore, 1977; Heaton, 1990; Ammann et al., 1999; Pearson et al., 2000; Savard et al., 2009; Redling et al., 2013; Felix & Elliott, 2014; Fibiger, 2014; Walters et al., 2015a, 2015b). We have excluded studies that infer NO_x $\delta^{15}N$ by measuring plant proxies or passive sampling in the environment (Ammann et al., 1999; Pearson et al.,2000; Savard et al. 2009; Redling et al., 2013; Felix & Elliott, 2014). This is because of equilibrium and kinetic isotope effects that can occur as NO_x reacts in the atmosphere to form NO_y, prior to NO_x deposition. In addition, the role vegetation plays in NO_x removal and atmospheric processes that mix the $\delta^{15}N$ of emission with the surroundings can also alter the $\delta^{15}N$ from the mobile source. Instead, we estimated the $\delta^{15}N$ value of NO_x emissions from vehicles only using studies that directly measured tailpipe NO_x emissions.

https://doi.org/10.5194/gmd-2020-322
Preprint. Discussion started: 22 December 2020

Geoscientific Model Development Discussions

There is a handful of NO_x $\delta^{15}N$ values measured from tailpipes, that span several decades. Moore (1977) collected 3 samples of tailpipe NO_x from one vehicle at different loads and engine speeds, which had $\delta^{15}N$ values of 3.7 ± 0.3 ‰. Heaton (1990) collected 8 samples from the tailpipes of 6 vehicles, on a testbed and on-road with different load and engine speeds. The resulting $\delta^{15}N$ values spanned -13 ‰ to 2 ‰, with an average of -7.5 ± 4.7 ‰. Neither Heaton nor Moore noted whether these 6 vehicles were equipped with any catalytic NO_x reduction technology, but it is unlikely since late 1970 and 80's s vehicles were seldomly equipped with catalytic NO_x reduction technology. Fibiger (2014) measured 5 samples of NO_x from diesel engines without SCR emitted into a smog chamber, the $\delta^{15}N$ values range from -19.2 ‰ to -16.7 ‰ (±0.97 ‰). The most comprehensive studies on vehicle NO_x $\delta^{15}N$ values are by Walters et al. (2015a, 2015 b). These studies were chosen to assign the $\delta^{15}N$ of NO_x emissions from vehicles in this study because these measurements were taken directly from vehicle tailpipes, rather than inferring them (i.e from roadside plant material, tree rings, or roadside NO_2) and had more samples (n = 73) compared to other studies. In addition, it measured gas and diesel vehicles separately, including those with and without three-way catalytic converter (TCC) and SCR technology. They also measured on-road and off-road vehicles separately. This research showed that the $\delta^{15}N$ of NO_x for vehicles without SCR or when SCR was not functioning was negative, at around -15‰. As SCRs warmed and became efficient at reducing NO_x the $\delta^{15}N$ value became less negative and even went positive. The measurements showed that the $\delta^{15}N$ values of NO_x emitted by gasoline on-road vehicle averages at -2.5 ± 1.5 ‰, and on-road diesel ranged from -5 ‰ to 0 ‰.

The emission rate of $^{15}NO_x$ from the mobile source was determined by Eq. 4 grid by grid, according to the contributions from on-road gasoline vehicles and on-road diesel vehicles, as well as their corresponding $\delta^{15}N$ values of these two types of vehicles grid by grid. NO_x emissions from off-road vehicles are regarded as area sources in SMOKE, which were processed over each county. In contrast, NO_x emissions from on-road vehicles are regarded as the mobile source in SMOKE, which will be processed along each highway. Each grid emission rate of $^{15}NO_x$ was assigned based on the contributions from gasoline and diesel vehicles, as well as the relative $\delta^{15}N$ values. The $\delta^{15}N$ of on-road gasoline vehicles (-2.7 ± 0.8 ‰) was based on the average of the vehicle travel time within each region with the same zip code (Walters et al., 2015b).

$$^{15}NO_x\ (mobile) = \left(\frac{\delta^{15}N_{NO_x\ (on-road\ gas)}}{1000} + 1\right) \times 0.0036 \times {}^{14}NO_x\ (on-road\ gas) + \left(\frac{\delta^{15}N_{NO_x\ (on-road\ diesel)}}{1000} + 1\right) \times 0.0036 \times {}^{14}NO_x\ (on-road\ diesel) \quad \text{Eq. (4)}$$

$$\text{Where } \delta^{15}N_{NO_x\ (on-road\ gas)} = -12.35 + 3.02 \times \ln(t + 0.455)$$

2.3 Point source of NO_x emission

The main NEI sectors for large amount of anthropogenic NO_x emissions that are located at a fixed, stationary position are categorized as NO_x point sources. These include NO_x emitted by fugitive dust and power plants. Fugitive dust does not significantly contribute to point NO_x emissions, so our inventory focused on power plants (Houyoux, 2005). Power plants were separated into two different types: EGU (electric generating units) and Non-EGU (e.g. commercial and industrial combustions). The emissions from EGUs account for 50-55% of the point source NO_x emissions, while non-EGUs account for 45-50%.

The $\delta^{15}N$ value of NO_x emitted from power plants have been estimated to vary from -19.7 ‰ to 25.6 ‰ (Heaton, 1987; Heaton, 1990; Snape, 2003; Felix et al., 2012; Felix et al., 2015; Walters et al., 2015b; Savard et al., 2017). We have ignored studies that measured $\delta^{15}N$ of NO_3^- or HNO_3

https://doi.org/10.5194/gmd-2020-322
Preprint. Discussion started: 22 December 2020

Geoscientific Model Development Discussions

from EGUs (Felix et al., 2015, Savard et al., 2017) and instead, only consider those studies that directly measured $\delta^{15}N$ of NO_x. Heaton (1990) collected 5 samples from the different coal-fired power stations with wall-fired and tangentially-fired boilers, at different power of 48, 500, and 600 MW. The $\delta^{15}N$ values of NO_x emissions from these measurements range from 6 ‰ to 13 ‰, with a standard deviation of 2.9 ‰. Snape (2003) measured 36 samples from power plants using three different types of coals in combustion chars in a drop tube reactor. The $\delta^{15}N$ values of NO_x ranged from 2.1 ‰ to 7.2 ‰, with a standard deviation of 1.37 ‰. The most comprehensive study on coal-fired power plants' NO_x values was by Felix et al. (2012). They measured the $\delta^{15}N$ values of NO_x emission from the coal-fired power stations with and without different emission control technologies. 16 coal-fired power plants with SCR, 3 coal-fired power plants with SNCR, 15 coal-fired power plants with OFA/LNB, and 8 coal-fired power plants without emission control technology were measured. The $\delta^{15}N$ values of NO_x emissions from these 42 measurements range from 9 ‰ to 25.6 ‰, with a standard deviation of 4.51 ‰. The NO_x $\delta^{15}N$ values when different emission control technologies were used varied: the $\delta^{15}N$ values of NO_x emissions from coal-fired power plants with SCR range from 15.5 ‰ to 25.6 ‰, those with SNCR ranged from 13.6 ‰ to 15.1 ‰, and those with OFA/LNB ranged from 9.0 ‰ to 12.6 ‰. The $\delta^{15}N$ values of NO_x emissions from coal-fired power plants without emission control technology range from 9.6 ‰ to 11.7 ‰, with a standard deviation of 0.79 ‰. According to Xing et al. (2013), about half of the coal-fired power plants in the United States are equipped with SCR. Thus, we assume 15 ‰ for the NO_x emissions from coal-fired power plants, which is the average between SCR and other emission control technologies.

The most comprehensive study on natural gas-fired NO_x values (Walters et al. 2015) collected 12 flue samples on the rooftop of a house from the ventilation pipe of a natural gas low-NO_x burner residential furnace without NO_x emission control technology. They also collected 11 flue samples from a sampling-port directly above a natural gas low-NO_x burner power plant. The measurement showed that the $\delta^{15}N$ values of NO_x emitted by natural gas power plants average -16.5 ± 1.7 ‰, which we used for the NO_x emission from natural gas power plants. The reason for using these values because they were measurements taken directly from the exhaust pipes, rather than inferring from downwind area or from rain samples, emitted by natural gas power plants, and included power plants with and without SCR technology. The latitude, longitude, and point sources characteristics (EGU and non-EGU, coal-fired or natural gas-fired, implementation of emission control technology) of each power plant was obtained from the US Energy Information Administration (2017). The power plants were assigned grids by their latitudes and longitudes, and the $\delta^{15}N$ values were assigned to these grids based on their emission characteristics, before determining the emission rate of $^{15}NO_x$ from point source using Eq. (2) and (3).

2.4 Area source of NO_x emission

Area sources are the stationary anthropogenic NO_x emissions that spread over a spatial extent and individually too small in magnitude to report as point sources. These include NO_x emitted by off-road vehicles, residential combustion (anthracite coal, bituminous coal, distillate oil, residual oil, natural gas, liquified petroleum gas, and wood), industrial processes (chemical manufacturing, food, and kindred products, metal production, mineral processes, petroleum refining, wood products, construction, machinery, mining, and quarrying, etc), agriculture production (crops, fertilizer application, livestock, animal waste, etc), solvent utilization, storage and transport, waste disposal, treatment, and recovery, forest wildfires, as well as road dust and fugitive dust. Among

https://doi.org/10.5194/gmd-2020-322
Preprint. Discussion started: 22 December 2020

Geoscientific Model Development Discussions

these, livestock and off-road vehicles are dominant, accounting for nearly 90% of area NO_x emissions across the contiguous United States (Houyoux, 2005). The annual area emissions from the NEI sectors were estimated at the county level and evenly divided into hourly emissions over the 12 km × 12 km grid for use in chemical transport modeling.

The area NO_x $\delta^{15}N$ values were based on the assumption that livestock waste and off-road vehicles (utility vehicles for agricultural and residential purposes) accounted for total area sources. Livestock waste NO_x $\delta^{15}N$ values were taken from Felix & Elliott (2014) since it is currently the only study about the $\delta^{15}N$ value of NO_x livestock waste emissions. They placed passive sampler with ventilation fans in an open-air and closed room in barns of cows and turkeys, respectively. The $\delta^{15}N$ values of NO_x emissions from these measurements range from -29 ‰ to -8.5 ‰. Among these samples, the $\delta^{15}N$ of NO_x emissions from turkey waste averages at -8.5 ‰, the $\delta^{15}N$ of NO_x emissions from cow waste averages at -24.7 ‰. We used -18.8 ‰ as the values of $\delta^{15}N$ values for NO_x emissions from livestock waste, which is the weighted average of the $\delta^{15}N$ of NO_x from turkey waste and cow waste emissions, roughly based on the population of turkey and cows on farms across the United States. We used the $\delta^{15}N$ values from Walters et al. (2015b) to estimate the $\delta^{15}N$ value of NO_x emissions from the off-road vehicle since it is the latest in detail study that measured the $\delta^{15}N$ value of NO_x specifically from the off-road vehicle. They collected 45 samples from the tailpipe of 9 different off-road vehicles (gasoline and diesel) with and without SCR, and before and after the sufficient engine warm-up times. The measurement showed that the $\delta^{15}N$ values of NO_x emitted by gasoline-powered off-road vehicle averaged -11.5 ± 2.7 ‰, diesel off-road vehicles without SCR averaged -19 ‰ ± 2 ‰, and diesel off-road vehicle with SCR averaged -2 ‰ ± 8 ‰. The emission rate of $^{15}NO_x$ from area source was determined by Eq. 5 grid by grid, according to the contributions from waste, off-road gasoline vehicle, and off-road diesel vehicle, as well as their corresponding $\delta^{15}N$ values based on previous researches.

$$
\begin{aligned}
{}^{15}NO_x\ (area) = {} & \left(\frac{\delta^{15}N_{NO_x\ (waste)}}{1000} + 1\right) \times 0.0036 \times {}^{14}NO_x\ (waste) \\
& + \left(\frac{\delta^{15}N_{NO_x\ (off-road\ gas)}}{1000} + 1\right) \times 0.0036 \times {}^{14}NO_x\ (off-road\ gas) \\
& + \left(\frac{\delta^{15}N_{NO_x\ (off-road\ diesel)}}{1000} + 1\right) \times 0.0036 \times {}^{14}NO_x\ (off-road\ diesel)
\end{aligned}
\qquad \text{Eq. (5)}
$$

The county-level annual $^{14}NO_x$ emission for the Midwestern US from NEI was converted to the dataset with hourly $^{14}NO_x$ emission over 12 × 12 km grids throughout the year. During this process, different NEI emission sectors were treated differently. Livestock waste and off-road vehicles were regarded as area sources by SMOKE, of which the $^{14}NO_x$ emission over each county was evenly divided into the grids. Power plants were regarded as the point source by SMOKE, of which the $^{14}NO_x$ emission from these facilities was located into the corresponding grids according to their latitudes and longitudes. On-road vehicles were regarded as the mobile source by SMOKE, of which the $^{14}NO_x$ emission along the roadways was estimated by MOBILE model, based on vehicle classifications, emission types, road type, fuel type, ambient temperature, and the number of vehicles along each roadway during each hour, before evenly dividing NO_x emission along each roadway into groups of 12 × 12 km grids. The soil was regarded as the biogenic source by SMOKE, of which the $^{14}NO_x$ emission produced by microbial nitrification and denitrification was estimated by BEIS model, based on land use type, normalized emission factor of NO_x, land cover, temperature, precipitation, fertilizer application, crop growing season, and crop canopy coverage during the growing season, over each 12 × 12 km grid. Then, the $^{15}NO_x$ emission of each SMOKE

https://doi.org/10.5194/gmd-2020-322
Preprint. Discussion started: 22 December 2020

Geoscientific Model Development Discussions

processing category was incorporated into the dataset based on the $\delta^{15}N$ values from previous research (Table 1) and Eq. (2-5).

$$\delta^{15}N_{NO_x\,(total)} = \left(\frac{\frac{^{15}NO_x\,(area)+{}^{15}NO_x\,(biog)+{}^{15}NO_x\,(mobile)+{}^{15}NO_x\,(point)}{^{14}NO_x\,(area)+{}^{14}NO_x\,(biog)+{}^{14}NO_x\,(mobile)+{}^{14}NO_x\,(point)}}{0.0036} - 1\right) \times 1000 \qquad \text{Eq. (6)}$$

https://doi.org/10.5194/gmd-2020-322
Preprint. Discussion started: 22 December 2020

Geoscientific Model Development Discussions

3. Results and Discussion

3.1 Simulated spatial variability of NO_x emission rates

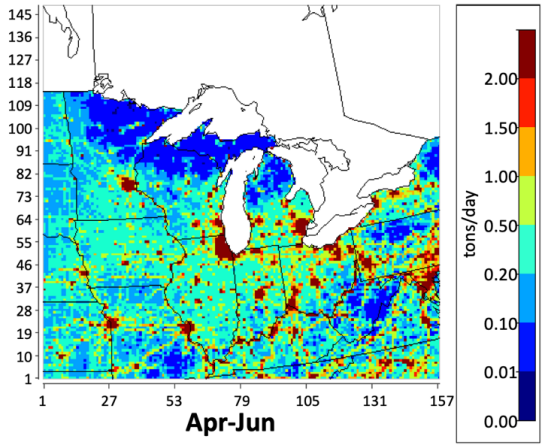

Figure 2: Total NO_x emission in the Midwest between April and June in tons/day. High NO_x emissions are associated with major urban areas such as Chicago, Detroit, Minneapolis-St Paul, Kansas City, St. Louis, Indianapolis, and Louisville.

We first examine the spatial heterogeneity of the NO_x emission rate for a single time period to illustrate the overall pattern of NO_x emission over the domain (Fig. 2). This is because the $\delta^{15}N$ value of total NO_x emission is determined by the fraction of each NO_x source (Eq. 6), which in turn is a function of their emission rates. Since our NO_x emissions are gridded by SMOKE using the NEI, they are by definition correct with respect to the NEI. However, a brief discussion of the salient geographic distribution of NO_x emissions and comparisons with other studies is warranted for completeness and as a backdrop for the discussion of NO_x fractions and resulting $\delta^{15}N$ values. We have arbitrarily chosen to sum the NO_x emissions during the April to June time period for this discussion.

The seasonal average NO_x emissions within the geographic domain during April to June range from less than 0.01 tons N/day to more than 15 tons N/day, with the seasonal grid average of 0.904 tons/day. The average NO_x emission over the 12 × 12 km grids simulated by SMOKE agrees well with estimates in previous studies, which was between 0.81 and 1.02 tons/day over the grids with the same size as this research but for the United States nationwide (Dignon & Hameed, 1989; Farrell et al., 1999; Selden et al., 1999; Xing et al, 2012). Within 75% of the grids within the geographic domain, the NO_x emissions are relatively low, ranging from between 0 and 0.5 tons/day (Fig. S1). Geographically, these grids are located in rural areas some distance away from metropolitan areas and highways (Fig. 2). The NO_x emission within about 20% of the grids is relatively moderate, ranging between 0.5 and 2.0 tons/day (Fig. S1). Geographically, these grids are mainly located along major highways and areas with medium population densities (Fig. 2). Urban centers comprise about 5% of the grids within the geographic domain and these have high

https://doi.org/10.5194/gmd-2020-322
Preprint. Discussion started: 22 December 2020

Geoscientific Model Development Discussions

NO_x emissions rates, ranging between 2.0 and 15.0 tons/day (Fig. S1). The metropolitan area's average is 5.03 tons/day, which is nearly 14 times of the average emission rate over the rest of the grids within the geographic domain (0.37 tons/day) due to high vehicle density associated with high population densities. The highest emissions rates are located within large cities (Fig. 2), such as Chicago, Detroit, Minneapolis-St Paul, Kansas City, St. Louis, Indianapolis, and Louisville, as well as the edge of the east coast metropolitan area (dark red). Summing the NO_x emissions among the grids that encompass these major midwestern cities, yields city-level NO_x emission rates that vary from 61.2 tons/day (Louisville, KY) to 634.1 tons/day (Chicago, IL). These city-level NO_x emission rate simulated by SMOKE (Table 2) agrees well with estimates derived from the Ozone Monitoring Instrument (OMI) in a previous study (Lu et al., 2015). Grids containing power plants are the significant NO_x hotspots within the geographic domain. These account for less than 1% of the grids within the geographic domain, but the NO_x emissions from a single grid that contains a power plant could be as high as 93.4 tons/day. Geographically, the power plants are mainly located along the Ohio River valley, near other water bodies, and often close to metropolitan areas (Fig. 2). The NO_x emission rates of the major power plants within the Midwest simulated by SMOKE (Table 3) match well with the measurement from Continuous Emission Monitoring System (CEMS) (de Foy et al., 2015; Duncan et al., 2013; Kim et al., 2009).

The geographic distribution of grid-level annual NO_x emission density in our simulation agrees with the county-level annual NO_x emission density discussed in the 2002 NEI booklet (Fig. S2; USEPA, 2018). For both grid-level emission density simulated by SMOKE and county-level emission density estimated by NEI, the relatively low values (less than 2.5 tons/mile^2) occur in the rural areas, especially located in the states of Minnesota, Iowa, Missouri, as well as the Plains states on the western edge of the domain. Similarly, the relatively moderate values (between 2.5 tons/mile^2 and 7.5 tons/mile^2) occur in the grids or counties that contain major highways; and the relatively high values (greater than 12.5 tons/mile^2) occurs in the grids or counties within metropolitan areas or in the grids or counties that contain power plants. Comparing the maps in different schemes, in addition, to show the geographic distribution of NO_x emission density at different levels, the map of grid-level NO_x emission density clearly shows locations of the objects with relatively high resolution, such as highways and power plant, as well as the more precise geographical range of metropolitan areas. The map of grid-level total NO_x emission provides a clear view of spatial variation, and show the geographic location of major cities, highways, and power plants, while it has obvious limitations. First, some power plants share the same grids with metropolitan areas or highways, which also has relatively high NO_x emission. As a result, it is hard to determine the dominant source for these grids. Similarly, among the grid with relatively low NO_x emission, the map of total NO_x emission cannot reveal the dominant source over these areas. In order to explore the composition of NO_x emission, the $\delta^{15}N$ value of total NO_x emission is necessary.

Urban Area	SMOKE-simulated emission rate		OMI-derived emission rate
	tons/day	tons/hr	tons/hr
Chicago, IL	634.074	24.42	23.3±9.7
Detroit, MI	288.617	12.026	18.7±7.8
Indianapolis, IN	72.487	3.021	3.1±1.3

https://doi.org/10.5194/gmd-2020-322
Preprint. Discussion started: 22 December 2020

Geoscientific Model Development Discussions

Kansas City, MO	150.733	6.281	5.1±2.1
Louisville, KY	61.178	2.549	2.5±1.0
Minneapolis, MN	220.957	9.207	9.3±3.9
St. Louis, MO	99.953	4.165	4.9±2.0

Table 2: The seasonal average NO_x emission rate for major cities in the Midwest

Power Plant Site	SMOKE-simulated emission rate tons/day	CEMS-measured emission rate	
		kt/yr	tons/day
Paradise, KY	93.414	38.33	105.014
New Madrid, MO	65.777	23.09	63.260
T. Hill Energy Center, MO	38.686	11.95	32.740
Kincaid, IL	38.934	11.92	32.644
Powerton, IL	62.394	21.56	59.068
Jeffrey Energy Center, KS	59.339	21.39	58.603

Table 3: The seasonal average NO_x emission rate for major power plants in the Midwest

https://doi.org/10.5194/gmd-2020-322
Preprint. Discussion started: 22 December 2020

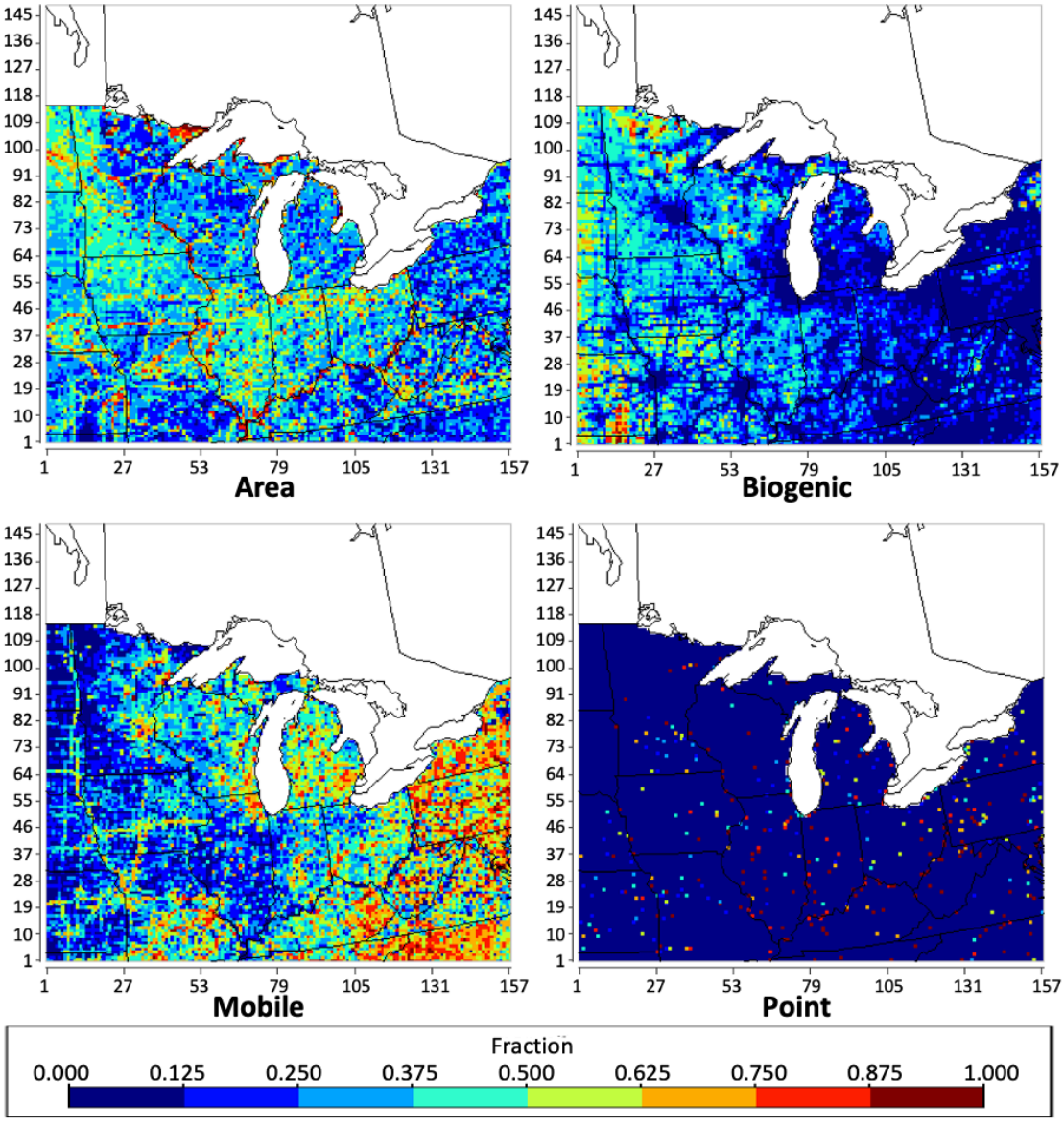

Figure 3: The geographical distribution of the fraction of NO_x emission from each SMOKE processing category (area, biogenic, mobile, point) over each grid throughout the Midwest between April and June based on NEI-2002.

https://doi.org/10.5194/gmd-2020-322
Preprint. Discussion started: 22 December 2020

Geoscientific Model Development Discussions
Open Access
EGU

We next examine the spatial heterogeneity of the NO_x fraction from each source category (Fig. 3) for the same time period (April to June). Since the $\delta^{15}N$ value of total NO_x is determined by the fractions of each NO_x emission source over each grid (Eq. 6), it is important to understand where in the domain these fractions differ and why. The area sources, which mainly consist of off-road vehicles, agriculture production, residential combustion, as well as the industrial processes, which are individually too low in magnitude to report as point sources, are fairly uniform in their distribution across the domain. The SMOKE simulation shows that NO_x emissions from area sources contribute an average NO_x emission fraction (f_{area}) of 0.271 for total NO_x emission and 0.290 for anthropogenic NO_x emission within the Midwest from April to June. This is slightly higher than the fraction of 0.279 for annual anthropogenic NO_x emissions over the Continental United States, estimated by 2002 NEI (USEPA, 2018). The fractions of NO_x emission from area sources over each grid cell within the geographic domain show a clear spatial variation. The area sources account for NO_x emission fractions ranging from 0.125 to 0.5 over about 75% of the grids within the geographic domain (Fig. S3). Geographically, the grids with relatively higher f_{area} are located in the rural area away from highways, especially in the states of Indiana, Illinois, Iowa, Minnesota, and Ohio, where agricultural is the most common land use classification. In the states of Wisconsin and Missouri, the f_{area} is slightly lower due to the higher fraction of NO_x emission from biogenic sources (f_{biog}). In the states of Pennsylvania and Michigan, the f_{area} is slightly lower due to the higher fraction of NO_x emission from mobile sources (f_{mobile}). In addition, the grids with f_{area} greater than 0.75 are mainly located along the Mississippi River and Ohio River, where the demand for water consumption and wastewater discharging from agriculture production could be satisfied.

The fraction of biogenic NO_x (f_{biog}) that are predominately by-products of microbial nitrification and denitrification occurring in soil, shows the clear spatial variation and is highest (from April to June) in the western portion of the domain (Fig. 3). The SMOKE simulation estimates that the fraction of biogenic NO_x emission averages 0.065 within the Midwest from April to June. The biogenic NO_x fraction is less than 0.5 in more than 90% of the grids within the geographic domain (Fig. S3). Geographically, the grids with relatively high f_{biog} are located in the western regions of the Midwest, away from cities and highways, in the states of Minnesota, Iowa, Missouri, Wisconsin, and Illinois, where the density of agricultural acreage and natural vegetation is higher than other states. Furthermore, within regions with higher f_{biog}, the obvious low f_{biog} values occur in the megacities and along the highways, which agrees well with the land-use related to the biogenic emission.

The SMOKE simulation shows that the NO_x emissions from mobile sources contribute to the fraction (f_{mobile}) of 0.325 for total NO_x emission and 0.347 for anthropologic NO_x emission within the Midwest from April to June, which is slightly lower than the fraction of 0.380 for annual anthropologic NO_x emission over the Continental United States, estimated by 2002 NEI (USEPA, 2018). The fractions of NO_x emission from the mobile source over each grid cell within the geographic domain show a clear spatial variation. The value of f_{mobile} within the geographic domain distributes evenly on the histogram (Fig. S3). Geographically, the grids with relatively higher f_{mobile} are located in major metropolitan regions and along the highways, where vehicles have the highest density, especially in the states of Pennsylvania, New York, Virginia, West Virginia, and North Carolina. In addition, within the states with lower f_{mobile}, the obvious high f_{mobile} values occur in the megacities and along the highways, which agrees well with the vehicle activities (US Census Bureau, n.d.).

https://doi.org/10.5194/gmd-2020-322
Preprint. Discussion started: 22 December 2020

Geoscientific Model Development Discussions

The point sources consist mainly of EGUs, as well as commercial and industrial processes involving combustion. Based on the SMOKE simulation, the NO_x emission from point sources contributes to the fraction (f_{point}) of 0.339 for total NO_x emission and 0.363 for anthropologic NO_x emission within the Midwest from April to June, which is slightly higher than the fraction of 0.343 for annual anthropologic NO_x emission over the Continental United States, estimated by 2002 NEI (USEPA, 2018). The fractions of NO_x emission from the point source over each grid cell within the geographic domain show a clear spatial variation. Geographically, the NO_x emission from point sources is dominant at the grids, where the power plants are located, mainly along the Ohio River valley and near other water bodies close to metropolitan areas. The point sources have no contribution to the NO_x emission among about 96% of the grids within the geographic domain. The rest of the 4% of the grids within the geographic domain are the locations of power plants. About 1/4 of the power plants are not at the same grids as highways, thus these grids have a fraction of at least 0.9 NO_x emission from point sources. Whereas the other 3/4 of the power plants share the same grids with highways, thus the point sources become relatively less dominant, due to the dilution by the NO_x emission from mobile sources.

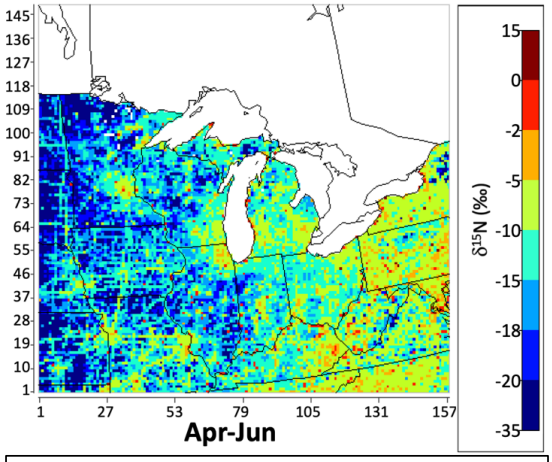

Figure 4: The $\delta^{15}N$ values of NO_x emission during April-June are presented by color in each grid. The warmer the color, the higher $\delta^{15}N$ values of NO_x emission.

Using these NO_x emission source fractions in each grid, the $\delta^{15}N$ values of NO_x were simulated. We then examine the spatial heterogeneity of $\delta^{15}N$ values of NO_x for a single time period and interpret them in terms of changes if NO_x emission fractions over the domain. The predicted $\delta^{15}N$ values of NO_x range from -35 ‰ to +15 ‰, with the seasonal average over the Midwest of -13.18 ‰ during the April to June period. The $\delta^{15}N$ value of total NO_x emissions in the Midwest during the April to June period has a significant spatial variation (Fig. 4). This can be qualitatively explained based on which emission source is dominant in a particular grid cell or grouping of cells in a certain region. The NO_x $\delta^{15}N$ model clearly shows the locations of big cities such as Chicago, Detroit, Minneapolis-St Paul, Kansas City, St. Louis, Indianapolis, and Louisville (gold and green). Likewise, major highways that connect these cities are obvious features (also gold and green), particularly on the western side of the domain. This is a consequence of the fact that in both cities and on major roads, on-road vehicles are the dominant NO_x source with assigned

https://doi.org/10.5194/gmd-2020-322
Preprint. Discussion started: 22 December 2020

$\delta^{15}N$ values of -2.5 ‰. In these grids, the NO_x $\delta^{15}N$ typically ranges from -5 to -10 ‰. Likewise, in the western part of the domain in the Midwest-Plains state region, where urban centers and population density is sparse and power plants are less numerous, soil emissions, with a $\delta^{15}N$ value of -34.3‰, control the NO_x budget. The predicted NO_x $\delta^{15}N$ values in these areas are very negative (dark blue), ranging from -20 to -34‰. In other grids, there are mixtures of sources such as mobile and biogenic leading to $\delta^{15}N$ values in the negative teens (aqua color), which is a mixture between the agricultural and urban NO_x sources. Similarly, the very positive $\delta^{15}N$ grids (~ +15 ‰) are located in grids that contain major power plants that dominate the NO_x emission budget (red and dark red), such as the Ohio River valley and West Virginia. These results show that there should be strong regional dependence on NO_x $\delta^{15}N$ values in the Midwestern United States.

https://doi.org/10.5194/gmd-2020-322
Preprint. Discussion started: 22 December 2020

Geoscientific Model Development Discussions
Open Access
EGU

3.2 Seasonal variation in $\delta^{15}N$ of NO_x

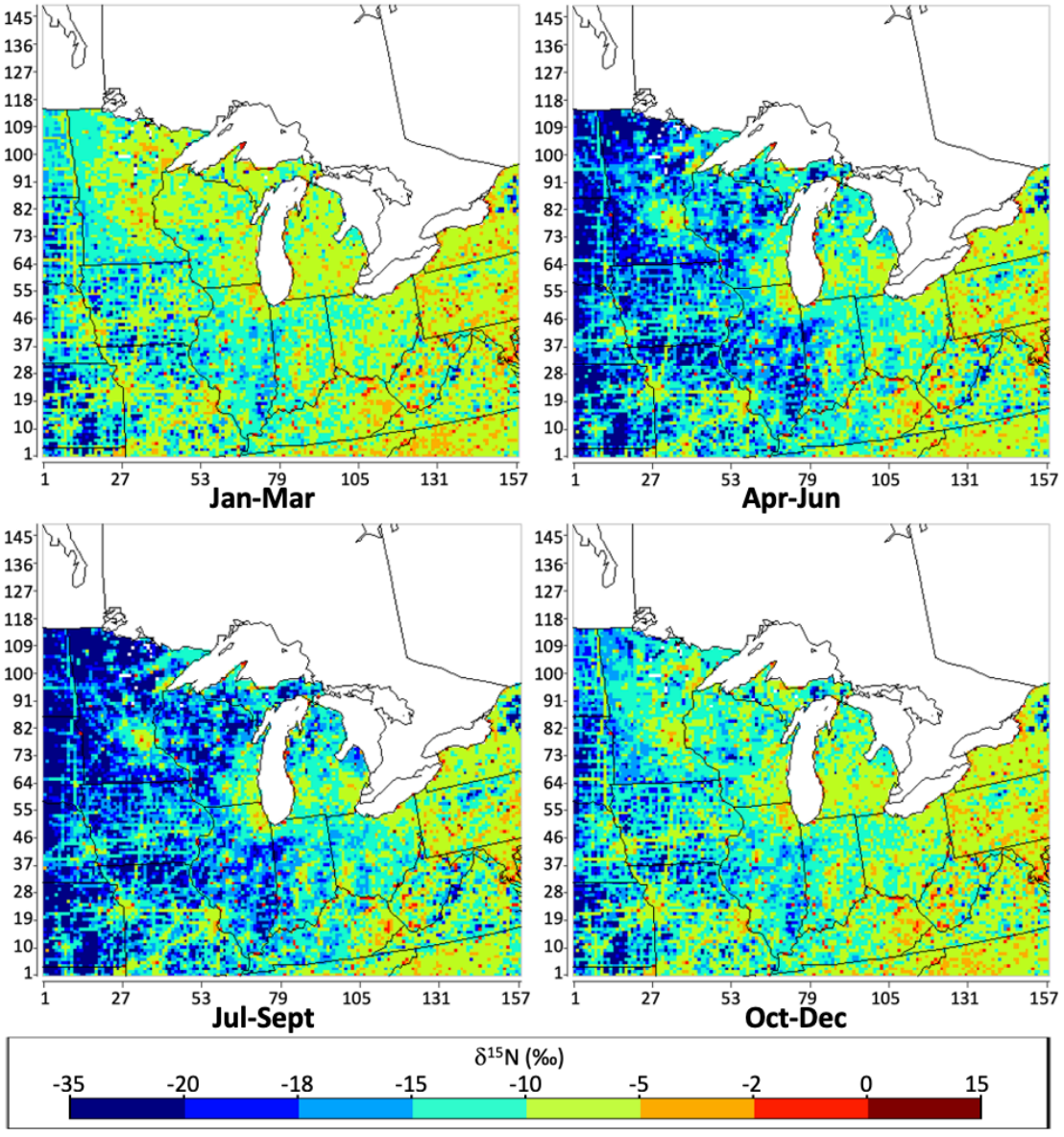

Figure 5: The geographical distribution of the $\delta^{15}N$ value of total NO_x emissions in each season (Winter: Jan-Mar; Spring: Apr-Jun; Summer: Jul-Sep; Fall: Oct-Dec) in per mil (‰) throughout the Midwest simulated by SMOKE, based on NEI-2002.

We next examine the temporal heterogeneity of NO_x $\delta^{15}N$ values over the domain and interpret them in terms of changes if NO_x emission fractions as a function of time. The predicted $\delta^{15}N$ value of total NO_x emissions in the Midwest during each season shows a significant temporal

https://doi.org/10.5194/gmd-2020-322
Preprint. Discussion started: 22 December 2020

Geoscientific Model Development Discussions

variation (Fig. 5). The $\delta^{15}N$ values of NO_x range from -35 ‰ to 15 ‰, with the annual average over the Midwest at -6.15 ‰. The maps for different seasons show the obvious changes in $\delta^{15}N$ values over western regions of the Midwest, from green ($\delta^{15}N$ = -15 ~ -5 ‰) to dark blue (-35 ~ -15 ‰) during the month from April to October.

In order to qualitatively analyze the changes in $\delta^{15}N(NO_x)$ among each season, the distributions of $\delta^{15}N(NO_x)$ among the same cut-offs as the maps on Fig. 5 were shown in the histograms (Fig. S4). The grids with $\delta^{15}N(NO_x)$ between -35‰ and -18‰ increase dramatically from less than 10% during fall (Oct-Dec) and winter (Jan-Mar) to more than 20% during spring (Apr-Jun) and summer (Jul-Sep). The grids with $\delta^{15}N(NO_x)$ between -18‰ and -2‰ decrease from around 90% during fall and winter to around 75% during spring and summer. In addition, the distribution of $\delta^{15}N(NO_x)$ shifts to lower values during spring and summer.

The significant temporal variation in the $\delta^{15}N$ value of total NO_x during different seasons can be quantitatively explained by changing fractions of NO_x emission from the biogenic source in any grid (Fig. 6) using Eq. (6). Unlike other NO_x emission source (figure not shown), the fraction of NO_x emission from biogenic sources changes significantly among each season within the geographic domain, especially over the rural areas of the states of Minnesota, Iowa, Missouri, Wisconsin, Illinois, Indiana, Kentucky, Michigan, and Ohio (Fig. 6). The fraction of NO_x emission from biogenic sources over these areas increases from less than 0.25 to more than 0.50 during the month from April to October, which is the growing season of the plant. During this period, the surface temperature and precipitation are relatively higher. As a result, the canopy coverage of the plants becomes higher, which leads to the increase of the NO_x emission from biogenic sources (Pierce, 2001; Vukovich & Pierce, 2002; Schwede et al., 2005; Pouliot & Pierce, 2009; USEPA, 2018). Besides this, the fertilizer application during this period is also responsible for the increase in soil NO_x emission (Li & Wang, 2008; Felix & Elliott, 2014).

In order to qualitatively analyze the changes in the fraction of NO_x emission from biogenic sources among each season, the distributions of the fractions among the same cut-offs as the maps on Fig. 6 were shown in the histograms (Fig. S5). Comparing the distributions of the fractions of NO_x emission from biogenic sources among the histograms for each season, the effects from the increasing of biogenic NO_x emission during the growing season of plants are clearly shown. In general, the distribution of the fraction shifts to higher values during spring (Apr-Jun) and summer (Jul-Sep), indicating the increase of biogenic emission. As a result, the distribution of $\delta^{15}N(NO_x)$ shifts to lower values during the same period (Fig. 5). The percentage of the grids with the fraction of biogenic emission less than 0.125 decreases dramatically from more than 50% during fall (Oct-Dec) and winter (Jan-Mar) to less than 35% during spring (Apr-Jun) and summer (Jul-Sep). As the NO_x emission from biogenic source becomes dominant, the percentage of the grids with $\delta^{15}N(NO_x)$ between -35‰ and -18‰ increases, while the percentage of the grids with $\delta^{15}N(NO_x)$ between -18‰ and -2‰ decreases, which sufficiently explains the trends shown on Fig. 5.

https://doi.org/10.5194/gmd-2020-322
Preprint. Discussion started: 22 December 2020

Geoscientific Model Development Discussions
Open Access
EGU

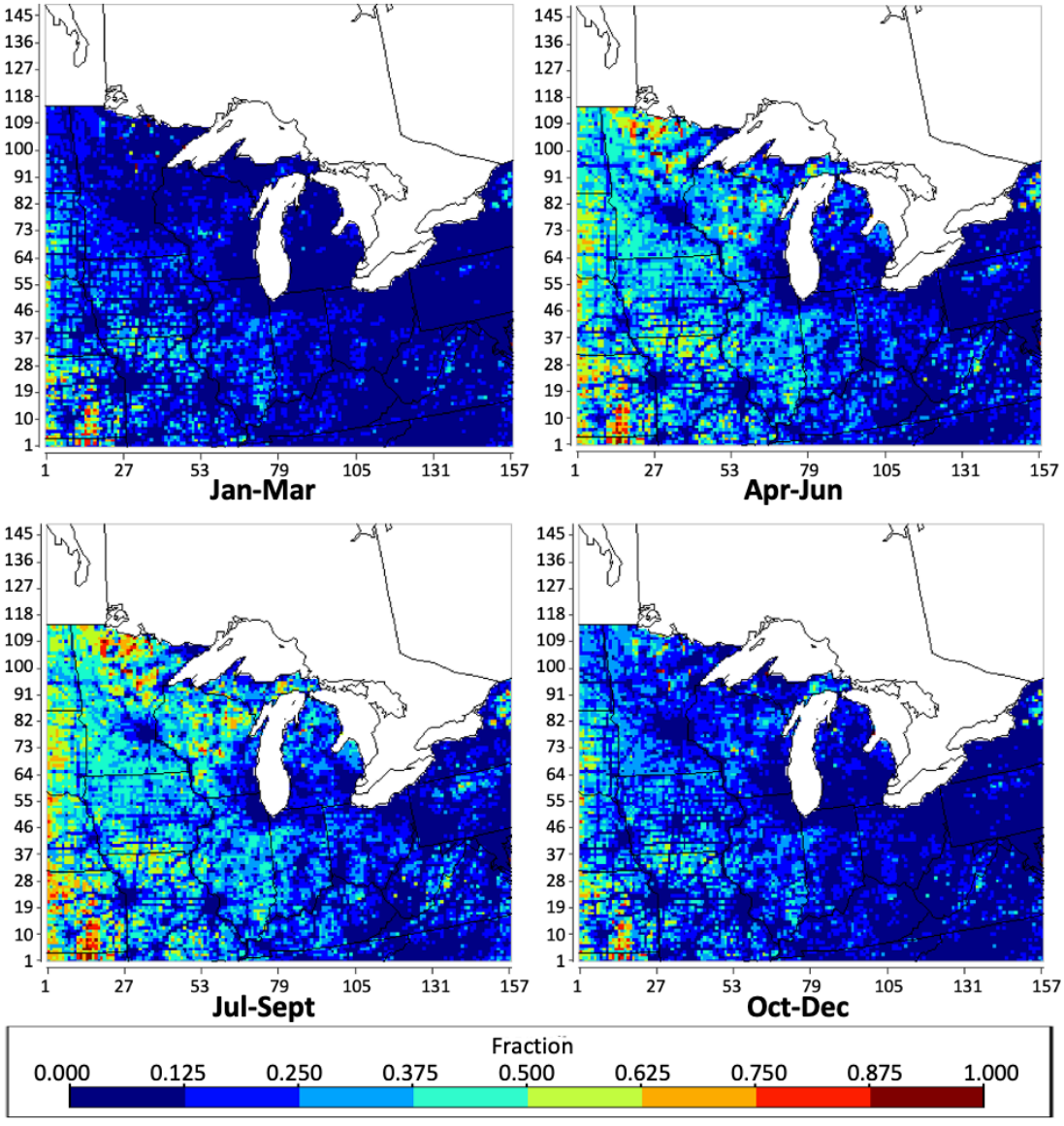

Figure 6: The geographical distribution of the fraction of NO_x emission from biogenic sources over each grid in each season (Winter: Jan-Mar; Spring: Apr-Jun; Summer: Jul-Sep; Fall: Oct-Dec) throughout the Midwest simulated by SMOKE, based on NEI-2002.

3.3 Different versions of emission inventories

The NO_x budget estimated by different versions (years) of the emission inventory varies. In order to compare the spatial heterogeneity of the fraction of NO_x from each source category for different emission inventory versions, the same analysis was done on the 2016 version of NEI (Fig.

https://doi.org/10.5194/gmd-2020-322
Preprint. Discussion started: 22 December 2020

Geoscientific Model Development Discussions

7). Overall, the anthropologic NO_x emission in the 2016 NEI is lower than in 2002, whereas the NO_x emission from biogenic emission is higher, especially in the western part of the domain. The difference in temperature, precipitation, fertilizer application, and crop canopy coverage during the crop growing season, as well as the adjustments of the algorithms for different versions of BEIS, potentially cause the variation in the fraction of NO_x emission from biogenic sources. The fraction of NO_x emission from area source in the 2016 NEI was lower than 2002 NEI for most of the grids within the domain, except the hotspots in West Virginia, northern Michigan, and eastern Kansas. The 2016 fraction of NO_x emission from the mobile source was lower than the 2002 NEI for most of the grids, especially in the eastern part of the domain. The fraction of NO_x emission from point source based on 2016 NEI shows fewer hotspots comparing 2002 NEI, which indicates less amount of power plant operated within the domain. The implementation of NO_x emission control technologies (SCR, SCNR, LNB, OFA), as well as the adjustments of the algorithms for different versions of MOBILE and MOVES, potentially cause the variation in the fraction of NO_x emission from anthropologic sources. Due to the significantly higher fraction of NO_x emission from biogenic source (Fig. S6) comparing to the estimation from 2002 NEI, the $\delta^{15}N$ value of total NO_x based on 2016 NEI was lower (Fig. S7).

https://doi.org/10.5194/gmd-2020-322
Preprint. Discussion started: 22 December 2020

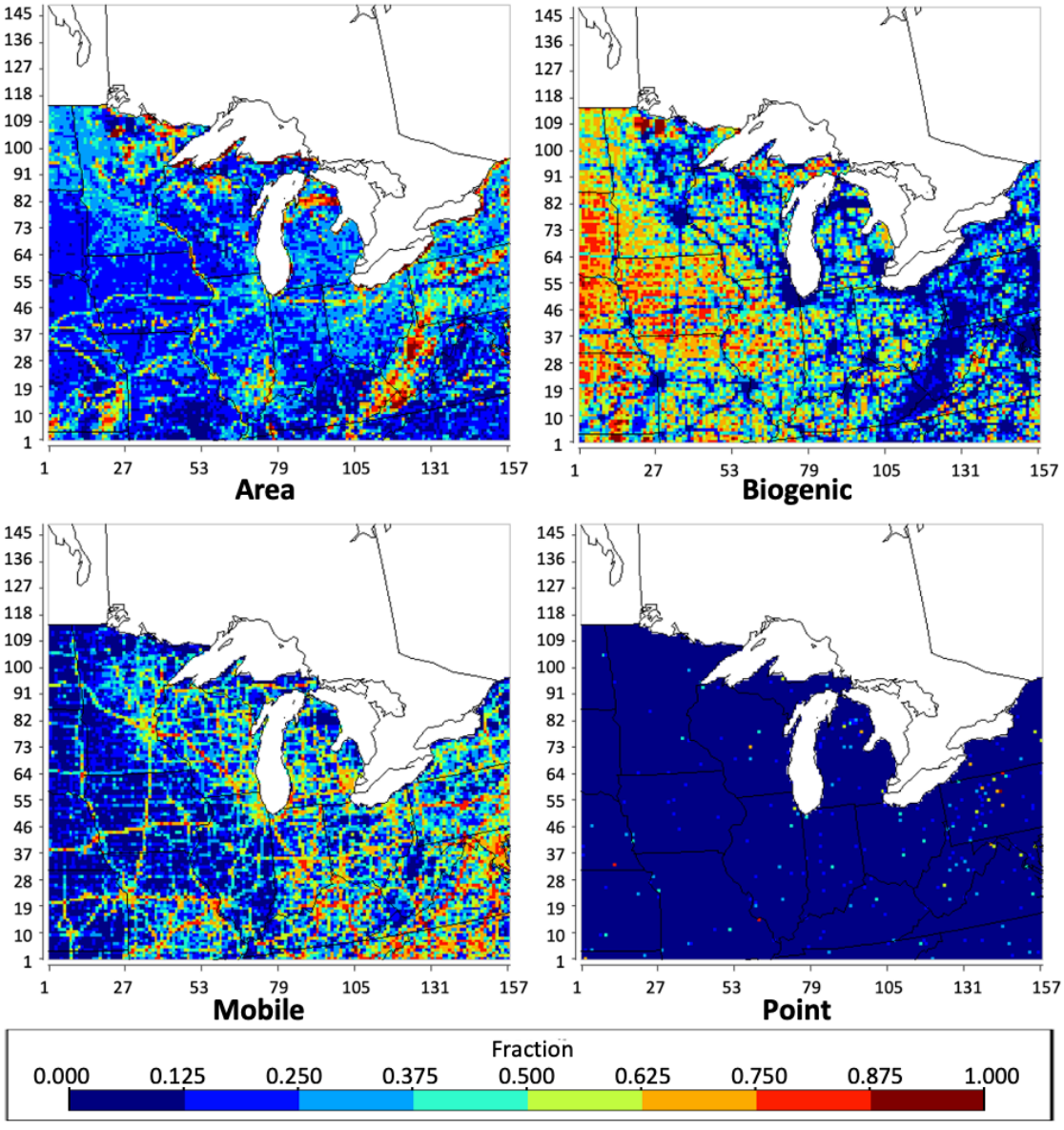

Figure 7: The geographical distribution of the fraction of NO_x emission from each SMOKE processing category (area, biogenic, mobile, point) over each grid throughout the Midwest between April and June, based on NEI-2016.

https://doi.org/10.5194/gmd-2020-322
Preprint. Discussion started: 22 December 2020

Geoscientific Model Development Discussions

3.4 Model-observation comparison

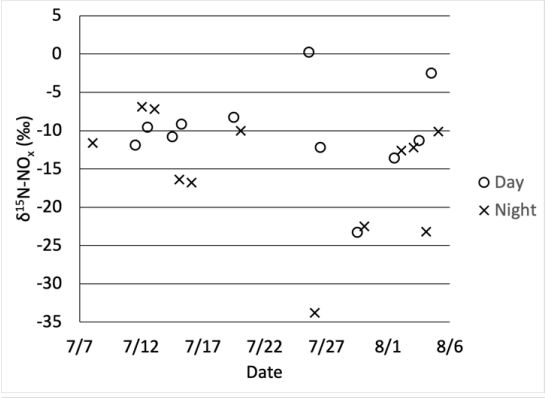

Figure 8: The $\delta^{15}N(NO_x)$ values measured at West Lafayette, IN between July 9 and August 5, 2016, from 8 am to 4 pm during the daytime (○), and from 9:30 pm to 5:30 am during the nighttime (×)

In order to evaluate the SMOKE simulation of Midwestern $\delta^{15}N(NO_x)$ values, they were compared to several existing observational datasets. The first comparison is to the only direct measurements of $\delta^{15}N(NO_x)$ within the domain, which occurred in West Lafayette, IN (Walters, Fang, & Michalski, 2018). The West Lafayette, IN site is in the northwest part of Indiana and is an NADP (National Atmospheric Deposition Program) site and home to Purdue University. 30 NO_x samples were collected using denuder tubes between July 8 and August 5, 2016 (Fig. 8) from 8 am to 4 pm during the daytime, and from 9:30 pm to 5:30 am during the nighttime. The measured $\delta^{15}N$ values of NO_x in West Lafayette ranged from -23.3 to 0.2 ‰ during the daytime and ranged from -33.8 to -6.9 ‰ during the nighttime.

https://doi.org/10.5194/gmd-2020-322
Preprint. Discussion started: 22 December 2020

Geoscientific Model Development Discussions

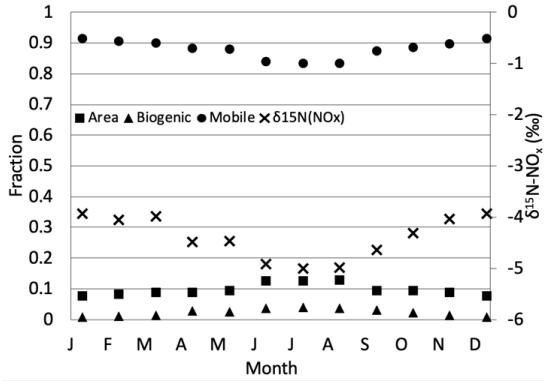

Figure 9: Fraction of monthly total NO_x emission by each SMOKE processing category (area [■], biogenic [▲], mobile [●]), and the monthly $\delta^{15}N$ values of total NO_x emission over the 12-km grid (right axis) over the 12-km grid that covers West Lafayette, IN simulated by SMOKE, based on NEI-2002.

The simulated $\delta^{15}N$ values of NO_x in West Lafayette show trivial monthly variations, and a small 1‰ seasonal trend (Fig. 9, right axis). The simulation shows that the $\delta^{15}N$ values stay around -4 ‰ from January to March, start to decrease in April until reaching -5 ‰ in June, and then start to increase in September until returning to -4 ‰ in November. These $\delta^{15}N(NO_x)$ reflect that in West Lafayette mobile (on-road vehicle) is the dominant NO_x source (Fig. 9, left axis). The NO_x fraction from the mobile sector was between 0.8 and 0.9 throughout the year. Mobile NO_x during summer is 10 % lower than average, which could be explained by the decrease in vehicle traffic during the summer holiday, when most students return to their home and when biogenic and area sources slightly increase due to peak agriculture activity. This seasonal change in fractions results in the -1‰ over the summer period.

https://doi.org/10.5194/gmd-2020-322
Preprint. Discussion started: 22 December 2020

Geoscientific Model Development Discussions

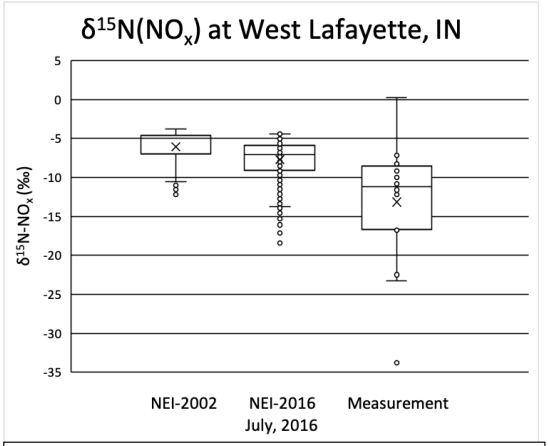

Figure 10: The distributions of $\delta^{15}N(NO_x)$ values over the 12-km grid that covers West Lafayette, IN from July 8 to August 5, simulated by SMOKE, using NEI-2002 (left) and NEI-2016 (middle) as the input, compare with the corresponding measurement (right) taken on July to August in 2016 (box: lower quartile, median, upper quartile; whisker: lower extreme, upper extreme; dots outside the whisker: outliers)

The SMOKE simulation of $\delta^{15}N$ values in West Lafayette, IN was compared with the measurement (Walters, Fang, & Michalski, 2018) from July 8 to August 5, 2016 (Fig. 10). The range of SMOKE simulated $\delta^{15}N(NO_x)$ from NEI-2002 ranges from -12.2‰ to -3.8‰, which is within the range of the corresponding measurement (-33.8 ~ 0.2 ‰). Whereas, the median (-5.0 ± 2.2 ‰) of SMOKE simulated $\delta^{15}N(NO_x)$ is higher than the median (-11.2 ± 8.0 ‰) of the measured values. As mentioned in section 3.3, the estimation of NO_x emission from biogenic sources by NEI-2016 is higher than the estimation by NEI-2002. As a result, using the data in NEI-2016 as the input, SMOKE simulated $\delta^{15}N(NO_x)$ values are lower, with the median (-7.0 ± 2.4 ‰) and range (-18.4 ~ -4.4 ‰) closer to the corresponding measurement. By comparing the SMOKE simulated $\delta^{15}N(NO_x)$ with the corresponding measurements, the NO_x emission budget in West Lafayette, IN, estimated by NEI-2016 is more accurate. While, the SMOKE simulated $\delta^{15}N(NO_x)$ values in West Lafayette, IN, based on both versions of NEI are higher than the corresponding measurements. Therefore, the emission from the soil, livestock waste, off-road vehicles, and natural gas power plant might be underestimated, and/or the emission from the on-road vehicle and coal-fired power plant might be overestimated for both versions of NEI.

https://doi.org/10.5194/gmd-2020-322
Preprint. Discussion started: 22 December 2020

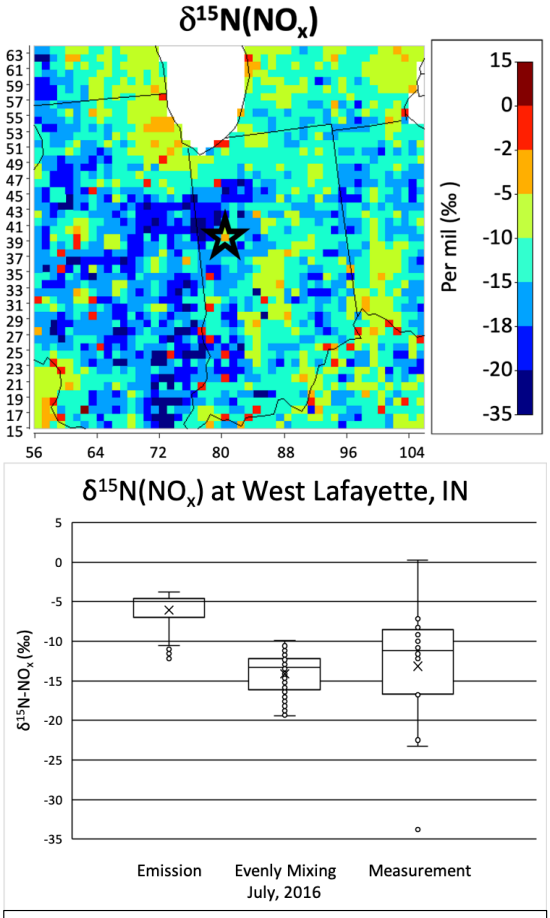

Figure 11: The $\delta^{15}N$ value of annual total NO_x emissions in 12 km^2 grids (top), center on West Lafayette, IN (☆). The modeled (with and without mixing) and measured $\delta^{15}N(NO_x)$ distributions for West Lafayette between from July 8 to August 5 (bottom). (box: lower quartile, median, upper quartile; whisker: lower extreme, upper extreme; dots outside the whisker: outliers)

In addition to the effects from NO_x emission sources, the lower values and greater variations in measured $\delta^{15}N(NO_x)$ might also be caused by the atmospheric mixing with the emission from surrounding grids, driven by the atmospheric processes. The map shows that the NO_x emission around West Lafayette is isotopically lighter than the neighborhood emission (Fig. 11). Thus, the mass-weighted average of the emission within 24 grids around West Lafayette, IN was used to calculate the $\delta^{15}N(NO_x)$ values, which considered the equal mixing of the emissions from the neighborhood, driven by 4 m/s of wind speed (National Centers for Environmental Information, 2019) during the 0.84 days of atmospheric NO_x lifetime (Stavrakou et al., 2013) (Eq. (7)). Using

https://doi.org/10.5194/gmd-2020-322
Preprint. Discussion started: 22 December 2020

Geoscientific Model Development Discussions
Open Access
EGU

this method, the simulated $\delta^{15}N$ values (median: -13.3 ± 2.5 ‰, range: -19.4 to -10.0 ‰) during the study period was closer to the measured values (median: -9.7 ± 7.6 ‰, range: -31.4 ~ 0.4 ‰) (Walters, Fang, & Michalski, 2018). Therefore, the $\delta^{15}N$ values are sensitive to effects from neighborhood emissions (Fig. 11). The more appropriate method will be tested on CMAQ (The Community Multiscale Air Quality Modeling System) in later researches, which takes the detailed atmospheric conditions into account for the atmospheric mixing of the pollutants.

$$(\delta^{15}N_{NO_x})_{total} = \sum f_{grid\,(i)} \times \delta^{15}N_{grid(i)} \quad \text{Eq. (7)}$$

https://doi.org/10.5194/gmd-2020-322
Preprint. Discussion started: 22 December 2020

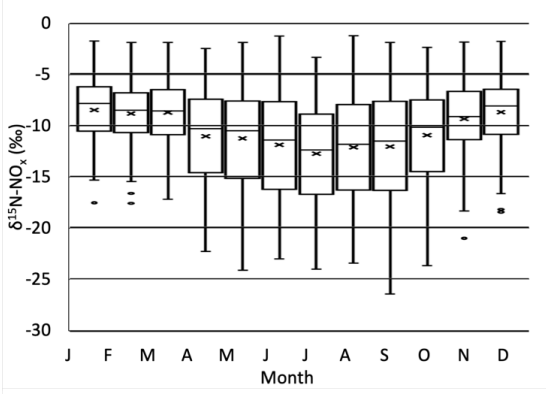

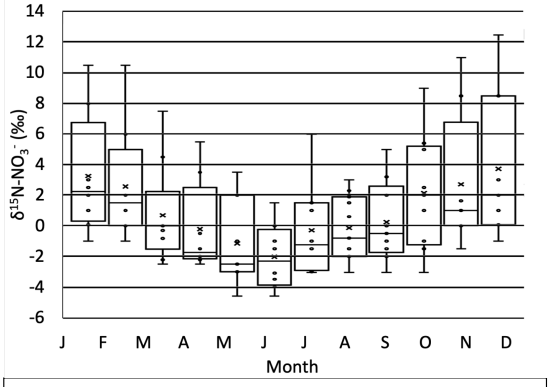

Figure 12: The SMOKE predicted $\delta^{15}N$ value of total NO_x at 82 NADP sites (top) using NEI-2002 compared to the measured $\delta^{15}N$ of rain NO_3^- (bottom) from prior studies.

Finally, we compared the emission model's predicted NO_x $\delta^{15}N$ values at 82 NADP sites in the Midwest (Fig. S8) with measurements of NO_3^- $\delta^{15}N$ values (Elliott et al., 2009; Garten, 1992; Hall et al., 2016; Occhipinti, 2008; Russell et al., 1998). The $\delta^{15}N$ values of NO_x simulated by SMOKE at these sites show large monthly variations and a seasonal trend (Fig. 12, top). The monthly boxes are the 1st and 3rd quantiles of the simulated monthly $\delta^{15}N$ of NO_x emissions at the 82 sites. The whiskers represent the minimum and maximum values without outliers. There is a wide range of $\delta^{15}N(NO_x)$ values within each month, with a minimum during March (-17.1~ -1.9 ‰) and a maximum during September (-26.5~-1.9 ‰). The seasonal trend shows low $\delta^{15}N(NO_x)$ during summer, with the median around -12 ‰, and high $\delta^{15}N(NO_x)$ during winter, with the median around -8 ‰. The SPSS analysis result shows the monthly change of $\delta^{15}N$ values is dominantly affected by biogenic emission. The effect from point sources is minimal since most of the NADP sites are more than 12 km (grid size of SMOKE) away from the power plant. The NADP sites are not in big cities but close to soil emission. Thus, biogenic emission has the strongest effect on the $\delta^{15}N$ values of NO_x emission, account for 86.6% of the change on $\delta^{15}N(NO_x)$.

Comparing with the SMOKE simulation, the measurements of $\delta^{15}N$ values of NO_3^- in the United States from previous researches (Elliott et al., 2009; Garten, 1992; Hall et al., 2016; Occhipinti, 2008; Russell et al., 1998) shows the similar monthly variations and seasonal trend

https://doi.org/10.5194/gmd-2020-322
Preprint. Discussion started: 22 December 2020

(Fig. 12, bottom). There is a wide range of $\delta^{15}N(NO_3^-)$ values within each month, with a minimum during June (-4.6~ 1.5 ‰) and a maximum during December (-1.0~12.5 ‰). The seasonal trend shows low $\delta^{15}N(NO_3^-)$ during summer, with the median around -2 ‰, and high $\delta^{15}N(NO_3^-)$ during winter, with the median around 2 ‰. The measured $\delta^{15}N$ values of NO_3^- has the same seasonal trend as the SMOKE simulated $\delta^{15}N$ values of NO_x. However, the measured $\delta^{15}N$ values of NO_3^- is about 10 ‰ higher than the SMOKE simulated $\delta^{15}N$ values of NO_x. This is because of the photochemical and equilibrium isotope effects that occur during the transformation of NO_x into NO_3^-, which enriches the ^{15}N isotopes in NO_3^-, as a more oxidized form of NO_y (Walters & Michalski, 2015; Walters et al., 2016). The 10‰ difference between the measured $\delta^{15}N(NO_3^-)$ and the SMOKE simulated $\delta^{15}N$ (NO_x) agree well with the previous study (Chang et al., 2018). The effect of tropospheric photochemistry, including the net N isotope effect during the conversion of NO_x to NO_3^-, will be addressed in subsequent papers.

4. Conclusion

The $\delta^{15}N$ of atmospheric NO_x was simulated by SMOKE, by considering the NO_x emissions from NEI emission sectors and the corresponding $\delta^{15}N$ values from previous researches. $\delta^{15}N$ is a decent tool to present the spatial and temporal composition of atmospheric NO_x, as well as the corresponding variation in NO_x emission sources. The simulation indicates that the NO_x emission from biogenic sources is the key driver for the variation of $\delta^{15}N$, especially among the NADP sites. Comparing with the measurements of $\delta^{15}N(NO_3^-)$ from NADP sites within the Midwest region, the simulated $\delta^{15}N$ agreed well with the seasonal trend and monthly variation. While, the simulated NO_x is slightly heavier than the corresponding measurements in West Lafayette, IN, taken from July to August 2016. According to the previous researches, the uncertainty of NO_x emission is 71-250% from soil and 10-15% from the vehicle. The variations among the removal efficiency of different emission control technologies vary from 30% to 90%, also causes the uncertainty of power plant NO_x emission. In addition, in this study, due to the lack of measurements, the $\delta^{15}N$ of coal-fired and natural gas non-EGUs (industrial boilers, commercial and residential fuel combustions) were assumed to be the same as the $\delta^{15}N$ of coal-fired and natural gas EGUs respectively. Thus, detailed measurements of the $\delta^{15}N$ of non-EGUs are necessary for future study. Besides this, the non-road vehicles (aircraft, ships, and trains) also need to be included in the future study.

If we only consider the effects from NO_x emission sources, the emission from soil, livestock waste, off-road vehicles, and natural gas power plant in West Lafayette, IN are possible to be underestimated, and the emission from the on-road vehicle and coal-fired power plant in West Lafayette, IN are possible to be overestimated. Another reason causing the estimated NO_x isotopically heavier than measured NO_x is the mixing caused by atmospheric processes, since the NO_x emission from the surrounding region of West Lafayette, IN is lighter. In addition, the tropospheric photochemistry could also alter the $\delta^{15}N$ values during the processes that convert NO_x to NO_y. The future work will explore the impacts of atmospheric processes and tropospheric photochemistry by incorporating ^{15}N into CMAQ and comparing the simulations with the corresponding measurements.

Data availability: The in-detail simulation results for $\delta^{15}N$ of NO_x emission based on 2002 and 2016 versions of National Emission Inventory and the associated python codes are achieved on Zenodo.org (10.5281/zenodo.4048992).

https://doi.org/10.5194/gmd-2020-322
Preprint. Discussion started: 22 December 2020

Author contributions: Huan Fang and Greg Michalski were the investigator for the project and organized the tasks. Huan Fang develop the model codes and performed the simulation to incorporate ^{15}N into SMOKE outputs and generated $\delta^{15}N$ values. Greg Michalski helped Huan Fang in interpreting the results. Huan Fang prepared the manuscript with contributions from all co-authors.

Acknowledgments: We would like to thank the Purdue Research Foundation and the Purdue Climate Change Research Center for providing funding for the project. We would like to thank Scott Spak from School of Urban & Regional Planning, University of Iowa for simulating SMOKE using NEI-2002. We would like to thank the CMAS (Community Modeling and Analysis System) Data Warehouse for providing SMOKE input and output datasets based on NEI-2016.

https://doi.org/10.5194/gmd-2020-322
Preprint. Discussion started: 22 December 2020

Geoscientific Model Development Discussions

References:

Almaraz, M., Bai, E., Wang, C., Trousdell, J., Conley, S., Faloona, I. and Houlton, B. Z.: Agriculture is a major source of NOx pollution in California, Sci. Adv., doi:10.1126/sciadv.aao3477, 2018.

Ammann, M., Siegwolf, R., Pichlmayer, F., Suter, M., Saurer, M. and Brunold, C.: Estimating the uptake of traffic-derived NO2 from 15N abundance in Norway spruce needles, Oecologia, doi:10.1007/s004420050710, 1999.

Beirle, S., Spichtinger, N., Stohl, A., Cummins, K. L., Turner, T., Boccippio, D., Cooper, O. R., Wenig, M., Grzegorski, M., Platt, U. and Wagner, T.: Estimating the NOx produced by lightning from GOME and NLDN data: A case study in the Gulf of Mexico, Atmos. Chem. Phys., doi:10.5194/acp-6-1075-2006, 2006.

Boersma, K. F., Eskes, H. J., Meijer, E. W. and Kelder, H. M.: Estimates of lightning NOx; production from GOME satellite observations, Atmos. Chem. Phys., doi:10.5194/acp-5-2311-2005, 2005.

Bradshaw, J., Davis, D., Grodzinsky, G., Smyth, S., Newell, R., Sandholm, S. and Liu, S.: Observed distributions of nitrogen oxides in the remote free troposphere from the NASA Global Tropospheric Experiment programs, Rev. Geophys., doi:10.1029/1999RG900015, 2000.

Chameides, W. L., Davis, D. D., Bradshaw, J., Rodgers, M., Sandholm, S. and Bai, D. B.: An estimate of the NO x production rate in electrified clouds based on NO observations from the GTE/CITE 1 fall 1983 field operation , J. Geophys. Res., doi:10.1029/jd092id02p02153, 1987.

Chang, Y., Zhang, Y., Tian, C., Zhang, S., Ma, X., Cao, F., Liu, X., Zhang, W., Kuhn, T. and Lehmann, M. F.: Nitrogen isotope fractionation during gas-to-particle conversion of NOx to NO3- in the atmosphere - Implications for isotope-based NO x source apportionment, Atmos. Chem. Phys., doi:10.5194/acp-18-11647-2018, 2018.

Christian, H. J., Blakeslee, R. J., Boccippio, D. J., Boeck, W. L., Buechler, D. E., Driscoll, K. T., Goodman, S. J., Hall, J. M., Koshak, W. J., Mach, D. M. and Stewart, M. F.: Global frequency and distribution of lightning as observed from space by the Optical Transient Detector, J. Geophys. Res. Atmos., doi:10.1029/2002jd002347, 2003.

Cicero-Fernândez, P., Long, J. R. and Winer, A. M.: Effects of Grades and Other Loads on On-Road Emissions of Hydrocarbons and Carbon Monoxide, J. Air Waste Manag. Assoc., doi:10.1080/10473289.1997.10464455, 1997.

Dameris, M., Grewe, V., Ponater, M., Deckert, R., Eyring, V., Mager, F., Matthes, S., Schnadt, C., Stenke, A., Steil, B., Brühl, C. and Giorgetta, M. A.: Long-term changes and variability in a transient simulation with a chemistry-climate model employing realistic forcing, Atmos. Chem. Phys., doi:10.5194/acp-5-2121-2005, 2005.

https://doi.org/10.5194/gmd-2020-322
Preprint. Discussion started: 22 December 2020

Davidson, E. A.: Pulses of nitric oxide and nitrous oxide flux following wetting of dry soil: an assessment of probable sources and importance relative to annual fluxes, Trace gas Exch. a Glob. Perspect., 1992.

Davidson, E. A. and Kingerlee, W.: A global inventory of nitric oxide emissions from soils, Nutr. Cycl. Agroecosystems, doi:10.1023/a:1009738715891, 1997.

de Foy, B., Lu, Z., Streets, D. G., Lamsal, L. N. and Duncan, B. N.: Estimates of power plant NOx emissions and lifetimes from OMI NO2 satellite retrievals, Atmos. Environ., doi:10.1016/j.atmosenv.2015.05.056, 2015.

De Laeter, J. R., Böhlke, J. K., De Bièvre, P., Hidaka, H., Peiser, H. S., Rosman, K. J. R. and Taylor, P. D. P.: Atomic weights of the elements: Review 2000 (IUPAC Technical Report), Pure Appl. Chem., doi:10.1351/pac200375060683, 2003.

DeCaria, A. J., Pickering, K. E., Stenchikov, G. L. and Ott, L. E.: Lightning-generated NOx and its impact on tropospheric ozone production: A three-dimensional modeling study of a Stratosphere-Troposphere Experiment: Radiation, Aerosols and Ozone (STERAO-A) thunderstorm, J. Geophys. Res. D Atmos., doi:10.1029/2004JD005556, 2005.

Dignon, J. and Hameed, S.: Global emissions of nitrogen and sulfur oxides from 1860 to 1980, J. Air Waste Manag. Assoc., doi:10.1080/08940630.1989.10466519, 1989.

Dreher, D. B. and Harley, R. A.: A fuel-based inventory for heavy-duty diesel truck emissions, J. Air Waste Manag. Assoc., doi:10.1080/10473289.1998.10463686, 1998.

Duncan, B. N., Yoshida, Y., De Foy, B., Lamsal, L. N., Streets, D. G., Lu, Z., Pickering, K. E. and Krotkov, N. A.: The observed response of Ozone Monitoring Instrument (OMI) NO2 columns to NOx emission controls on power plants in the United States: 2005-2011, Atmos. Environ., doi:10.1016/j.atmosenv.2013.08.068, 2013.

Elliott, E. M., Kendall, C., Boyer, E. W., Burns, D. A., Lear, G. G., Golden, H. E., Harlin, K., Bytnerowicz, A., Butler, T. J. and Glatz, R.: Dual nitrate isotopes in dry deposition: Utility for partitioning NO x source contributions to landscape nitrogen deposition, J. Geophys. Res. Biogeosciences, doi:10.1029/2008JG000889, 2009.

Elliott, E. M., Kendall, C., Wankel, S. D., Burns, D. A., Boyer, E. W., Harlin, K., Bain, D. J. and Butler, T. J.: Nitrogen isotopes as indicators of NOx source contributions to atmospheric nitrate deposition across the midwestern and northeastern United States, Environ. Sci. Technol., doi:10.1021/es070898t, 2007.

Farrell, A., Carter, R. and Raufer, R.: The NOx Budget: Market-based control of tropospheric ozone in the northeastern United States, Resour. Energy Econ., doi:10.1016/S0928-7655(98)00035-9, 1999.

https://doi.org/10.5194/gmd-2020-322
Preprint. Discussion started: 22 December 2020

Fehr, T., Höller, H. and Huntreiser, H.: Model study on production and transport of lightning-produced NOx in a EULINOX supercell storm, J. Geophys. Res. D Atmos., doi:10.1029/2003JD003935, 2004.

Felix, J. D., Elliott, E. M. and Shaw, S. L.: Nitrogen isotopic composition of coal-fired power plant NOx: Influence of emission controls and implications for global emission inventories, Environ. Sci. Technol., doi:10.1021/es203355v, 2012.

Felix, J. D. and Elliott, E. M.: The agricultural history of human-nitrogen interactions as recorded in ice core δ15N-NO3-, Geophys. Res. Lett., doi:10.1002/grl.50209, 2013.

Felix, J. D. and Elliott, E. M.: Isotopic composition of passively collected nitrogen dioxide emissions: Vehicle, soil and livestock source signatures, Atmos. Environ., doi:10.1016/j.atmosenv.2014.04.005, 2014.

Felix, J. D., Elliott, E. M., Avery, G. B., Kieber, R. J., Mead, R. N., Willey, J. D. and Mullaugh, K. M.: Isotopic composition of nitrate in sequential Hurricane Irene precipitation samples: Implications for changing NOx sources, Atmos. Environ., doi:10.1016/j.atmosenv.2015.01.075, 2015.

Fibiger, D. L., Hastings, M. G., Lew, A. F. and Peltier, R. E.: Collection of NO and NO2 for isotopic analysis of NOx emissions, Anal. Chem., doi:10.1021/ac502968e, 2014.

Fraser, A., Goutail, F., McLinden, C. A., Melo, S. M. L. and Strong, K.: Lightning-produced NO2 observed by two ground-based UV-visible spectrometers at Vanscoy, Saskatchewan in August 2004, Atmos. Chem. Phys., doi:10.5194/acp-7-1683-2007, 2007.

Fujita, E. M., Croes, B. E., Bennett, C. L., Lawson, D. R., Lurmann, F. W. and Main, H. H.: Comparison of emission inventory and ambient concentration ratios of CO, NMOG, and NOx in California's South Coast Air Basin, J. Air Waste Manag. Assoc., doi:10.1080/10473289.1992.10466989, 1992.

Fujita, E. M., Campbell, D. E., Zielinska, B. B., Sagebiel, J. C., Bowen, J. L., Goliff, W. S., Stockwell, W. R. and Lawson, D. R.: Diurnal and weekday variations in the source contributions of ozone precursors in California's South Coast Air Basin, J. Air Waste Manag. Assoc., doi:10.1080/10473289.2003.10466226, 2003.

Fujita, E. M., Stockwell, W. R., Campbell, D. E., Keislar, R. E. and Lawson, D. R.: Evolution of the magnitude and spatial extent of the weekend ozone effect in California's South Coast Air Basin, 1981–2000, J. Air Waste Manag. Assoc., doi:10.1080/10473289.2003.10466225, 2003.

Galbally, I. E. and Roy, C. R.: Loss of fixed nitrogen from soils by nitric oxide exhalation [11], Nature, doi:10.1038/275734a0, 1978.Gallardo, L. and Rodhe, H.: Oxidized nitrogen in the remote Pacific: The role of electrical discharges over the oceans, J. Atmos. Chem., doi:10.1023/A:1005738402496, 1997.

https://doi.org/10.5194/gmd-2020-322
Preprint. Discussion started: 22 December 2020

Gallardo, L. and Rodhe, H.: Oxidized nitrogen in the remote Pacific: The role of electrical discharges over the oceans, J. Atmos. Chem., doi:10.1023/A:1005738402496, 1997.

Galloway, J. N. and Cowling, E. B.: Reactive nitrogen and the world: 200 Years of change, in Ambio., 2002.

Galloway, J. N., Dentener, F. J., Capone, D. G., Boyer, E. W., Howarth, R. W., Seitzinger, S. P., Asner, G. P., Cleveland, C. C., Green, P. A., Holland, E. A., Karl, D. M., Michaels, A. F., Porter, J. H., Townsend, A. R. and Vörösmarty, C. J.: Nitrogen cycles: Past, present, and future, Biogeochemistry, doi:10.1007/s10533-004-0370-0, 2004.

Ganzeveld, L. N., Lelieveld, J., Dentener, F. J., Krol, M. C., Bouwman, A. J. and Roelofs, G. J.: Global soil-biogenic NOX emissions and the role of canopy processes, J. Geophys. Res. Atmos., doi:10.1029/2001JD001289, 2002.

Garten, C. T.: Nitrogen isotope composition of ammonium and nitrate in bulk precipitation and forest throughfall, Int. J. Environ. Anal. Chem., doi:10.1080/03067319208027017, 1992.

Gauss, M., Myhre, G., Isaksen, I. S. A., Grewe, V., Pitari, G., Wild, O., Collins, W. J., Dentener, F. J., Ellingsen, K., Gohar, L. K., Hauglustaine, D. A., Iachetti, D., Lamarque, J. F., Mancini, E., Mickley, L. J., Prather, M. J., Pyle, J. A., Sanderson, M. G., Shine, K. P., Stevenson, D. S., Sudo, K., Szopa, S. and Zeng, G.: Radiative forcing since preindustrial times due to ozone change in the troposphere and the lower stratosphere, Atmos. Chem. Phys., doi:10.5194/acp-6-575-2006, 2006.

Grell, G. A., Dudhia, J., & Stauffer, D. R.: A description of the fifth-generation Penn State/NCAR mesoscale model (MM5), NCAR Technical Note NCAR/TN-398+ STR, 1994.

Hall, S. J., Ogata, E. M., Weintraub, S. R., Baker, M. A., Ehleringer, J. R., Czimczik, C. I. and Bowling, D. R.: Convergence in nitrogen deposition and cryptic isotopic variation across urban and agricultural valleys in northern Utah, J. Geophys. Res. Biogeosciences, doi:10.1002/2016JG003354, 2016.

Hanson, P. J. and Lindberg, S. E.: Dry deposition of reactive nitrogen compounds: A review of leaf, canopy and non-foliar measurements, Atmos. Environ. Part A, Gen. Top., doi:10.1016/0960-1686(91)90020-8, 1991.

Harley, R. A., McKeen, S. A., Pearson, J., Rodgers, M. O. and Lonneman, W. A.: Analysis of motor vehicle emissions during the Nashville/Middle Tennessee Ozone Study, J. Geophys. Res. Atmos., doi:10.1029/2000JD900677, 2001.

Heaton, T. H. E.: 15N14N ratios of nitrate and ammonium in rain at Pretoria, South Africa, Atmos. Environ., doi:10.1016/0004-6981(87)90080-1, 1987.

Heaton, T. H. E.: 15N/14N ratios of NOx from vehicle engines and coal-fired power stations, Tellus B, doi:10.1034/j.1600-0889.1990.00007.x-i1, 1990.

https://doi.org/10.5194/gmd-2020-322
Preprint. Discussion started: 22 December 2020

Hoering, T.: The isotopic composition of the ammonia and the nitrate ion in rain, Geochim. Cosmochim. Acta, doi:10.1016/0016-7037(57)90021-2, 1957.

Houlton, B. Z., Boyer, E., Finzi, A., Galloway, J., Leach, A., Liptzin, D., Melillo, J., Rosenstock, T. S., Sobota, D. and Townsend, A. R.: Intentional versus unintentional nitrogen use in the United States: Trends, efficiency and implications, Biogeochemistry, doi:10.1007/s10533-012-9801-5, 2013.

Houyoux, M.: Clean Air Interstate Rule Emissions Inventory Technical Support Document. US EPA, 2005.

Hudman, R. C., Moore, N. E., Mebust, A. K., Martin, R. V., Russell, A. R., Valin, L. C. and Cohen, R. C.: Steps towards a mechanistic model of global soil nitric oxide emissions: Implementation and space based-constraints, Atmos. Chem. Phys., doi:10.5194/acp-12-7779-2012, 2012.

Huntrieser, H., Schlager, H., Feigl, C. and Höller, H.: Transport and production of NOX in electrified thunderstorms: Survey of previous studies and new observations at midlatitudes, J. Geophys. Res. Atmos., doi:10.1029/98JD02353, 1998.

Huntrieser, H., Feigl, C., Schlager, H., Schröder, F., Gerbig, C., van Velthoven, P., Flatøy, F., Théry, C., Petzold, A., Höller, H. and Schumann, U.: Airborne measurements of NOx, tracer species, and small particles during the European lightning nitrogen oxides experiment, J. Geophys. Res. Atmos., doi:10.1029/2000jd000209, 2002.

Ingalls, M. N.: On-road vehicle emission factors from measurements in a Los Angeles area tunnel, in Proceedings - A&WMA Annual Meeting., 1989.

Jacob, D. J. and Wofsy, S. C.: Budgets of reactive nitrogen, hydrocarbons, and ozone over the Amazon forest during the wet season, J. Geophys. Res., doi:10.1029/jd095id10p16737, 1990.

Jaeglé, L., Steinberger, L., Martin, R. V. and Chance, K.: Global partitioning of NOx sources using satellite observations: Relative roles of fossil fuel combustion, biomass burning and soil emissions, in Faraday Discussions., 2005.

Johansson, C.: Pine forest: a negligible sink for atmospheric NO x in rural Sweden , Tellus B Chem. Phys. Meteorol., doi:10.3402/tellusb.v39i5.15360, 1987.

Kim, S. W., Heckel, A., Frost, G. J., Richter, A., Gleason, J., Burrows, J. P., McKeen, S., Hsie, E. Y., Granier, C. and Trainer, M.: NO2 columns in the western United States observed from space and simulated by a regional chemistry model and their implications for NO x emissions, J. Geophys. Res. Atmos., doi:10.1029/2008JD011343, 2009.

Koike, M., Kondo, Y., Kita, K., Takegawa, N., Nishi, N., Kashihara, T., Kawakami, S., Kudoh, S., Blake, D., Shirai, T., Liley, B., Ko, M. K., Miyazaki, Y., Kawasaki, Z. and Ogawa, T.:

https://doi.org/10.5194/gmd-2020-322
Preprint. Discussion started: 22 December 2020

Measurements of reactive nitrogen produced by tropical thunderstorms during BIBLE-C, J. Geophys. Res. Atmos., doi:10.1029/2006JD008193, 2007.

Lawrence, M. G., Chameides, W. L., Kasibhatla, P. S., Levy, H. and Moxim, W.: Lightning and atmospheric chemistry: The rate of atmospheric NO production, in Handbook of Atmospheric Electrodynamics., 2017.

Lerdau, M. T., Munger, J. W. and Jacob, D. J.: The NO2 flux conundrum, Science (80-.)., doi:10.1126/science.289.5488.2291, 2000.

Levy, H., Moxim, W. J. and Kasibhatla, P. S.: A global three-dimensional time-dependent lightning source of tropospheric NOx, J. Geophys. Res. Atmos., doi:10.1029/96jd02341, 1996.

Li, D. and Wang, X.: Nitrogen isotopic signature of soil-released nitric oxide (NO) after fertilizer application, Atmos. Environ., doi:10.1016/j.atmosenv.2008.01.042, 2008.

Li, Y., Schichtel, B. A., Walker, J. T., Schwede, D. B., Chen, X., Lehmann, C. M. B., Puchalski, M. A., Gay, D. A. and Collett, J. L.: Increasing importance of deposition of reduced nitrogen in the United States, Proc. Natl. Acad. Sci. U. S. A., doi:10.1073/pnas.1525736113, 2016.

Lighty, J. A. S., Veranth, J. M. and Sarofim, A. F.: Combustion aerosols: Factors governing their size and composition and implications to human health, J. Air Waste Manag. Assoc., doi:10.1080/10473289.2000.10464197, 2000.

Lu, Z., Streets, D. G., De Foy, B., Lamsal, L. N., Duncan, B. N. and Xing, J.: Emissions of nitrogen oxides from US urban areas: Estimation from Ozone Monitoring Instrument retrievals for 2005-2014, Atmos. Chem. Phys., doi:10.5194/acp-15-10367-2015, 2015.

Ludwig, J., Meixner, F. X., Vogel, B. and Forstner, J.: Soil-air exchange of nitric oxide: An overview of processes, environmental factors, and modeling studies, Biogeochemistry, doi:10.1023/A:1006424330555, 2001.

Martin, R. V., Sauvage, B., Folkins, I., Sioris, C. E., Booone, C., Bernath, P. and Ziemke, J.: Space-based constraints on the production of nitric oxide by lightning, J. Geophys. Res. Atmos., doi:10.1029/2006JD007831, 2007.

Miller, D. J., Wojtal, P. K., Clark, S. C. and Hastings, M. G.: Vehicle NOx emission plume isotopic signatures: Spatial variability across the eastern United States, J. Geophys. Res., doi:10.1002/2016JD025877, 2017.

Miller, D. J., Chai, J., Guo, F., Dell, C. J., Karsten, H. and Hastings, M. G.: Isotopic Composition of In Situ Soil NOx Emissions in Manure-Fertilized Cropland, Geophys. Res. Lett., doi:10.1029/2018GL079619, 2018.

Moore, H.: The isotopic composition of ammonia, nitrogen dioxide and nitrate in the atmosphere, Atmos. Environ., doi:10.1016/0004-6981(77)90102-0, 1977.

https://doi.org/10.5194/gmd-2020-322
Preprint. Discussion started: 22 December 2020

Muller, J. F.: Geographical distribution and seasonal variation of surface emissions and deposition velocities of atmospheric trace gases, J. Geophys. Res., doi:10.1029/91JD02757, 1992.

Müller, J.-F. and Stavrakou, T.: Inversion of CO and NOx emissions using the adjoint of the IMAGES model, Atmos. Chem. Phys., doi:10.5194/acp-5-1157-2005, 2005.

Murray, L. T.: Lightning NOx and Impacts on Air Quality, Curr. Pollut. Reports, doi:10.1007/s40726-016-0031-7, 2016.

National Centers for Environmental Information: U.S. Wind Climatology, Available from: https://www.ncdc.noaa.gov/societal-impacts/wind/, 2019.

Occhipinti, C., Aneja, V. P., Showers, W. and Niyogi, D.: Back-trajectory analysis and source-receptor relationships: Particulate matter and nitrogen isotopic composition in rainwater, in Journal of the Air and Waste Management Association., 2008.

Ott, L. E., Pickering, K. E., Stenchikov, G. L., Huntrieser, H. and Schumann, U.: Effects of lightning NOx production during the 21 July European Lightning Nitrogen Oxides Project storm studied with a three-dimensional cloud-scale chemical transport model, J. Geophys. Res. Atmos., doi:10.1029/2006JD007365, 2007.

Parrish, D. D.: Critical evaluation of US on-road vehicle emission inventories, Atmos. Environ., doi:10.1016/j.atmosenv.2005.11.033, 2006.

Pearson, J., Wells, D. M., Seller, K. J., Bennett, A., Soares, A., Woodall, J. and Ingrouille, M. J.: Traffic exposure increases natural 15N and heavy metal concentrations in mosses, New Phytol., doi:10.1046/j.1469-8137.2000.00702.x, 2000.

Pierce, T. E.: Reconsideration of the Emission Factors assumed in BEIS3 for Three USGS Vegetation Categories: Shrubland, Coniferous Forest, and Deciduous Forest, 2001.

Pierson, W. R., Gertler, A. W. and Bradow, R. L.: Comparison of the scaqs tunnel study with other onroad vehicle emission data, J. Air Waste Manag. Assoc., doi:10.1080/10473289.1990.10466799, 1990.

Pierson, W. R., Gertler, A. W., Robinson, N. F., Sagebiel, J. C., Zielinska, B., Bishop, G. A., Stedman, D. H., Zweidinger, R. B. and Ray, W. D.: Real-world automotive emissions - summary of studies in the Fort McHenry and Tuscarora Mountain Tunnels, in Atmospheric Environment., 1996.

Pilegaard, K.: Processes regulating nitric oxide emissions from soils, Philos. Trans. R. Soc. B Biol. Sci., doi:10.1098/rstb.2013.0126, 2013.

https://doi.org/10.5194/gmd-2020-322
Preprint. Discussion started: 22 December 2020

Potter, C. S., Matson, P. A., Vitousek, P. M. and Davidson, E. A.: Process modeling of controls on nitrogen trace gas emissions from soils worldwide, J. Geophys. Res. Atmos., doi:10.1029/95JD02028, 1996.

Pouliot, G., & Pierce, T. E.: Integration of the Model of Emissions of Gases and Aerosols from Nature (MEGAN) into the CMAQ Modeling System, in: 18th International Emission Inventory Conference, Baltimore, Maryland, 14 April 2009, 14-17, 2009.

Redling, K., Elliott, E., Bain, D. and Sherwell, J.: Highway contributions to reactive nitrogen deposition: Tracing the fate of vehicular NOx using stable isotopes and plant biomonitors, Biogeochemistry, doi:10.1007/s10533-013-9857-x, 2013.

Ridley, B. A., Dye, J. E., Walega, J. G., Zheng, J., Grahek, F. E. and Rison, W.: On the production of active nitrogen by thunderstorms over New Mexico, J. Geophys. Res. Atmos., doi:10.1029/96jd01706, 1996.

Ridley, B., Ott, L., Pickering, K., Emmons, L., Montzka, D., Weinheimer, A., Knapp, D., Grahek, F., Li, L., Heymsfield, G., McGill, M., Kucera, P., Mahoney, M. J., Baumgardner, D., Schultz, M. and Brasseur, G.: Florida thunderstorms: A faucet of reactive nitrogen to the upper troposphere, J. Geophys. Res. D Atmos., doi:10.1029/2004JD004769, 2004.

Russell, K. M., Galloway, J. N., MacKo, S. A., Moody, J. L. and Scudlark, J. R.: Sources of nitrogen in wet deposition to the Chesapeake Bay region, Atmos. Environ., doi:10.1016/S1352-2310(98)00044-2, 1998.

Savard, M. M., Bégin, C., Smirnoff, A., Marion, J. and Rioux-Paquette, E.: Tree-ring nitrogen isotopes reflect anthropogenic NOx emissions and climatic effects, Environ. Sci. Technol., doi:10.1021/es802437k, 2009.

Savard, M. M., Cole, A., Smirnoff, A. and Vet, R.: Δ15N values of atmospheric N species simultaneously collected using sector-based samplers distant from sources – Isotopic inheritance and fractionation, Atmos. Environ., doi:10.1016/j.atmosenv.2017.05.010, 2017.

Sawyer, R. F., Harley, R. A., Cadle, S. H., Norbeck, J. M., Slott, R. and Bravo, H. A.: Mobile sources critical review: 1998 NARSTO assessment, Atmos. Environ., doi:10.1016/S1352-2310(99)00463-X, 2000.

Scholes, M. C., Martin, R., Scholes, R. J., Parsons, D. and Winstead, E.: NO and N2O emissions from savanna soils following the first simulated rains of the season, Nutr. Cycl. Agroecosystems, doi:10.1023/a:1009781420199, 1997.

Schumann, U., Kurz, C., Schlager, H., Huntrieser, H., Emmons, L., Labrador, L., Meijer, E., Ulanovsky, A. and Viciani, S.: Towards a robust estimate of the global lightning nitrogen oxides source rate and its error bound, in European Space Agency, (Special Publication) ESA SP., 2006.

https://doi.org/10.5194/gmd-2020-322
Preprint. Discussion started: 22 December 2020

Schumann, U. and Huntrieser, H.: The global lightning-induced nitrogen oxides source, Atmos. Chem. Phys., doi:10.5194/acp-7-3823-2007, 2007.

Schwartz, S. E.: The Whitehouse effect - Shortwave radiative forcing of climate by anthropogenic aerosols: An overview, J. Aerosol Sci., doi:10.1016/0021-8502(95)00533-1, 1996.

Schwede, D., Pouliot, G. and Pierce, T.: Changes to the biogenic emissions inventory system version 3 (BEIS3), in 4th Annual CMAS User's Conference., 2005.

Selden, T. M., Forrest, A. S., & Lockhart, J. E.: Analyzing the reductions in US air pollution emissions: 1970 to 1990, Land Economics, 1-21, doi: 10.2307/3146990, 1999.

Spak, S., Holloway, T., Mednick, A., & Stone, B.: Evaluation of Bottom-Up Mobile Emissions Inventories in the Upper Midwest, in: American Geophysical Union Fall Meeting, San Francisco, California, 10-14 Dec 2007, 2007.

Shepherd, M. F., Barzetti, S. and Hastie, D. R.: The production of atmospheric NOx and N2O from a fertilized agricultural soil, Atmos. Environ. Part A, Gen. Top., doi:10.1016/0960-1686(91)90277-E, 1991.

Singer, B. C. and Harley, R. A.: A Fuel-Based Motor Vehicle Emission Inventory, J. Air Waste Manag. Assoc., doi:10.1080/10473289.1996.10467492, 1996.

Singer, B. C. and Harley, R. A.: A fuel-based inventory of motor vehicle exhaust emissions in the Los Angeles area during summer 1997, Atmos. Environ., doi:10.1016/S1352-2310(99)00358-1, 2000.

Skamarock, W. C., Dye, J. E., Defer, E., Barth, M. C., Stith, J. L., Ridley, B. A. and Baumann, K.: Observational- and modeling-based budget of lightning-produced NOx in a continental thunderstorm, J. Geophys. Res. Atmos., doi:10.1029/2002jd002163, 2003.

Slovik, S., Siegmund, A., Fuhrer, H. W. and Heber, U.: Stomatal uptake of SO2, NOx and O3 by spruce crowns (Picea abies) and canopy damage in Central Europe, New Phytol., doi:10.1111/j.1469-8137.1996.tb01884.x, 1996.

Snape, C. E., Sun, C., Fallick, A. E., Irons, R. and Haskell, J.: Potential of stable nitrogen isotope ratio measurements to resolve fuel and thermal NOx in coal combustion, Fuel Chem. Div. Prepr., 2003.

Snyder, J. P.: Map projections - a working manual, US Geol. Surv. Prof. Pap., 1987.

Srivastava, R. K., Neuffer, W., Grano, D., Khan, S., Staudt, J. E. and Jozewicz, W.: Controlling NO x emission from industrial sources, Environ. Prog., doi:10.1002/ep.10063, 2005.

https://doi.org/10.5194/gmd-2020-322
Preprint. Discussion started: 22 December 2020

Staudt, A. C., Jacob, D. J., Ravetta, F., Logan, J. A., Bachiochi, D., Sandholm, S., Ridley, B., Singh, H. B. and Talbot, B.: Sources and chemistry of nitrogen oxides over the tropical Pacific, J. Geophys. Res. Atmos., doi:10.1029/2002jd002139, 2003.

Stavrakou, T., Müller, J. F., Boersma, K. F., Van Der A., R. J., Kurokawa, J., Ohara, T. and Zhang, Q.: Key chemical NOx sink uncertainties and how they influence top-down emissions of nitrogen oxides, Atmos. Chem. Phys., doi:10.5194/acp-13-9057-2013, 2013.

Stehfest, E. and Bouwman, L.: N2O and NO emission from agricultural fields and soils under natural vegetation: Summarizing available measurement data and modeling of global annual emissions, Nutr. Cycl. Agroecosystems, doi:10.1007/s10705-006-9000-7, 2006.

Stevenson, D. S., Dentener, F. J., Schultz, M. G., Ellingsen, K., van Noije, T. P. C., Wild, O., Zeng, G., Amann, M., Atherton, C. S., Bell, N., Bergmann, D. J., Bey, I., Butler, T., Cofala, J., Collins, W. J., Derwent, R. G., Doherty, R. M., Drevet, J., Eskes, H. J., Fiore, A. M., Gauss, M., Hauglustaine, D. A., Horowitz, L. W., Isaksen, I. S. A., Krol, M. C., Lamarque, J. F., Lawrence, M. G., Montanaro, V., Müller, J. F., Pitari, G., Prather, M. J., Pyle, J. A., Rast, S., Rodriquez, J. M., Sanderson, M. G., Savage, N. H., Shindell, D. T., Strahan, S. E., Sudo, K. and Szopa, S.: Multimodel ensemble simulations of present-day and near-future tropospheric ozone, J. Geophys. Res. Atmos., doi:10.1029/2005JD006338, 2006.

The Institute for the Environment - The University of North Carolina at Chapel Hill: SMOKE v4.5 User's Manual, Available from: https://www.cmascenter.org/smoke/documentation/4.5/html/, 2017.

Thoene, B., Rennenberg, H. and Weber, P.: Absorption of atmospheric NO2 by spruce (Picea abies) trees: II. Parameterization of NO2 fluxes by controlled dynamic chamber experiments, New Phytol., doi:10.1111/j.1469-8137.1996.tb04630.x, 1996.

Thomas, R. J., Krehbiel, P. R., Rison, W., Hamlin, T., Boccippio, D. J., Goodman, S. J. and Christian, H. J.: Comparison of ground-based 3-dimensional lightning mapping observations with satellite-based LIS observations in Oklahoma, Geophys. Res. Lett., doi:10.1029/1999GL010845, 2000.

Tie, X., Zhang, R., Brasseur, G. and Lei, W.: Global NOx production by lightning, J. Atmos. Chem., doi:10.1023/A:1016145719608, 2002.

Tost, H., Jöckel, P. and Lelieveld, J.: Lightning and convection parameterisations - Uncertainties in global modelling, Atmos. Chem. Phys., doi:10.5194/acp-7-4553-2007, 2007.

United States Census Bureau: 2007−2011 American Community Survey 5-Year Estimates, travel time to work by zip code, table B08303, Available from: https://www.census.gov/programs-surveys/acs/technical-documentation/table-and-geography-changes/2011/5-year.html, 2019.

United States Energy Information Administration: Electricity, Available from: https://www.eia.gov/electricity/data/eia860/, 2017.

https://doi.org/10.5194/gmd-2020-322
Preprint. Discussion started: 22 December 2020

Geoscientific Model Development Discussions

United States Environmental Protection Agency: National Emissions Inventory (NEI), Available from: https://www.epa.gov/air-emissions-inventories/national-emissions-inventory-nei, 2014.

United States Environmental Protection Agency: Biogenic Emissions Landuse Database, Available from: https://www.epa.gov/air-emissions-modeling/biogenic-emissions-landuse-database-version-3-beld3, 2018.

United States Environmental Protection Agency: 2002 National Emissions Inventory (NEI) Booklet, Available from: https://archive.epa.gov/epa/air-emissions-inventories/2002-national-emissions-inventory-nei-booklet.html, 2018

US Environmental Protection Agency: User's Guide to MOBILE6.1 and MOBILE6.2 Mobile Source Emission Factor Model, Tech. Rep. EPA420-R-03-010, 2003.

Van Noije, T. P. C., Eskes, H. J., Dentener, F. J., Stevenson, D. S., Ellingsen, K., Schultz, M. G., Wild, O., Amann, M., Atherton, C. S., Bergmann, D. J., Bey, I., Boersma, K. F., Butler, T., Cofala, J., Drevet, J., Fiore, A. M., Gauss, M., Hauglustaine, D. A., Horowitz, L. W., Isaksen, I. S. A., Krol, M. C., Lamarque, J. F., Lawrence, M. G., Martin, R. V., Montanaro, V., Müller, J. F., Pitari, G., Prather, M. J., Pyle, J. A., Richter, A., Rodriguez, J. M., Savage, N. H., Strahan, S. E., Sudo, K., Szopa, S. and Van Roozendael, M.: Multi-model ensemble simulations of tropospheric NO2 compared with GOME retrievals for the year 2000, Atmos. Chem. Phys., doi:10.5194/acp-6-2943-2006, 2006.

Vukovich, J., & Pierce, T.: The implementation of BEIS3 within the SMOKE modeling framework, in: Proceedings of the 11th International Emissions Inventory Conference, Atlanta, Georgia, 15 April 2002, 15-18, 2002.

Walters, W. W., Goodwin, S. R. and Michalski, G.: Nitrogen stable isotope composition (δ15N) of vehicle-emitted NOx, Environ. Sci. Technol., doi:10.1021/es505580v, 2015a.

Walters, W. W., Tharp, B. D., Fang, H., Kozak, B. J. and Michalski, G.: Nitrogen Isotope Composition of Thermally Produced NOx from Various Fossil-Fuel Combustion Sources, Environ. Sci. Technol., doi:10.1021/acs.est.5b02769, 2015b.

Walters, W. W. and Michalski, G.: Theoretical calculation of nitrogen isotope equilibrium exchange fractionation factors for various NOy molecules, Geochim. Cosmochim. Acta, doi:10.1016/j.gca.2015.05.029, 2015.

Walters, W. W., Simonini, D. S. and Michalski, G.: Nitrogen isotope exchange between NO and NO2 and its implications for δ15N variations in tropospheric NOx and atmospheric nitrate, Geophys. Res. Lett., doi:10.1002/2015GL066438, 2016.

Walters, W. W., Fang, H. and Michalski, G.: Summertime diurnal variations in the isotopic composition of atmospheric nitrogen dioxide at a small midwestern United States city, Atmos. Environ., doi:10.1016/j.atmosenv.2018.01.047, 2018.

https://doi.org/10.5194/gmd-2020-322
Preprint. Discussion started: 22 December 2020

Weber, P. and Rennenberg, H.: Dependency of nitrogen dioxide (NO2) fluxes to wheat (Triticum aestivum L.) leaves from NO2 concentration, light intensity, temperature and relative humidity determined from controlled dynamic chamber experiments, Atmos. Environ., doi:10.1016/1352-2310(96)00008-8, 1996.

Wong, S., Wang, W. C., Isaksen, I. S. A., Berntsen, T. K. and Sundet, J. K.: A global climate-chemistry model study of present-day tropospheric chemistry and radiative forcing from changes in tropospheric O3 since the preindustrial period, J. Geophys. Res. D Atmos., doi:10.1029/2003JD003998, 2004.

Xing, J., Pleim, J., Mathur, R., Pouliot, G., Hogrefe, C., Gan, C. M. and Wei, C.: Historical gaseous and primary aerosol emissions in the United States from 1990 to 2010, Atmos. Chem. Phys., doi:10.5194/acp-13-7531-2013, 2013.

Yan, X., Ohara, T. and Akimoto, H.: Statistical modeling of global soil NOX emissions, Global Biogeochem. Cycles, doi:10.1029/2004GB002276, 2005.

Yienger, J. J. and Levy, H.: Empirical model of global soil-biogenic NOx emissions, J. Geophys. Res., doi:10.1029/95jd00370, 1995.

Yu, Z. and Elliott, E. M.: Novel Method for Nitrogen Isotopic Analysis of Soil-Emitted Nitric Oxide, Environ. Sci. Technol., doi:10.1021/acs.est.7b00592, 2017.

Zörner, J., Penning de Vries, M. J. M., Beirle, S., Sihler, H., Veres, P. R., Williams, J. and Wagner, T.: Multi-satellite sensor study on precipitation-induced emission pulses of NO_x from soils in semi-arid ecosystems, Atmos. Chem. Phys. Discuss., doi:10.5194/acp-2016-93, 2016.